

DIATOMS Si UPTAKE CAPACITY DRIVES CARBON EXPORT IN COASTAL UPWELLING SYSTEMS

Abrantes F.^{1,2*}, Cermeno P.³, Lopes C.^{1,2}, Romero O.⁴, Matos, L.^{1,4}, Van Iperen J.⁵, Rufino M.¹ and Magalhães V.¹

1 - Portuguese Institute for the Ocean and Atmosphere, RuaAlferedoMagalhãesRamalho 6, 1495-006 Lisboa, Portugal. TM 351934309002, fatima.abrantes@ipma.pt

2 - Centro de Ciências do Mar (CCMAR--LA), Universidade do Algarve, Campus de Gambelas, 8005-139 Faro, Portugal

3 - Institute of Marine Sciences (ICM-CSIC), PasseioMarítim de la Barceloneta, 37-49. E-08003 Barcelona, Spain

4 - Center for Marine Environmental Sciences University of Bremen(MARUM), Leobener Str. D-28359 Bremen Germany

5 - Royal Netherlands Institute for Sea Research (NIOZ), Landsdiep 41797 SZ 't Horntje (Texel), The Netherlands

Physical Sciences; Earth, Atmospheric, and Planetary Sciences

Keywords: Diatoms; primary production, coastal upwelling,

ABSTRACT

Coastal upwelling systems account for about half of global ocean primary production and contribute disproportionately to biologically-driven carbon sequestration. Diatoms, silica-precipitating microalgae, constitute the dominant phytoplankton in these productive regions, and their abundance and assemblage composition in the sedimentary record is considered one of the best proxies for paleoproductivity. The study of the sedimentary diatom abundance (SDA) and total organic carbon content (TOC) in the five most important coastal upwelling systems of the modern ocean (Iberia-Canary, Benguela, Peru-Humboldt, California and Somalia-Oman) reveals a global scale positive relationship between diatom productivity and organic carbon burial. The analysis of SDA in conjunction with environmental variables of coastal upwelling systems such as upwelling strength, satellite-derived net primary production and surface water nutrient concentrations shows different relations between SDA and primary production on the regional scale and a global SDA modulated by the capacity of diatoms to take up silicic acid which ultimately sets an upper limit to global export production in these ocean regions.

SIGNIFICANCE STATEMENT

Diatoms (siliceous algae) are the dominant primary producers of the most productive ($\pm 50\%$ world's primary production) and best fishing areas (20% world's catch) of the modern ocean, the coastal upwelling systems.

Their role as a biological pump, linking the silicate and the carbon biogeochemical cycles, turns them important players on climate change.

A comparison of long-term worldwide diatom sedimentary abundance (SDA) to environmental variables can help untangle their response to a warming climate.

We found a regional variance of the relation SDA-primary production and a worldwide covariance of SDA and sedimentary organic carbon. A key role of silicate for the global SDA distribution pattern emerges as a function of the diatoms physiological capacity to uptake Si from the upwelled waters.

INTRODUCTION

Coastal upwelling zones exist along the eastern boundary currents of the Atlantic and Pacific Oceans. In these areas, alongshore equatorward winds and the Coriolis effect force surface waters to diverge offshore, giving rise to the upwelling of nutrient-rich deep waters into the surface. The five most important coastal upwelling systems of the modern ocean are associated to: (1) the Canary Current off northwest Africa including its extension to the Iberian Peninsula (Iberia-Canary); (2) the Benguela current along southwest Africa; (3) the Peru-Humboldt current off western south America (SE Pacific); (4) the California Current off western N America (NE Pacific) and the Somalia-Oman monsoon derived upwelling off the Arabian Peninsula (1, 2). At present, 80 to 90% of oceanic primary production, which represents 50% of Earth's primary production, occurs in the $\pm 1\%$ of the ocean characterized by coastal upwelling (2, 3).

The potential role of coastal upwelling systems on carbon uptake and export turns their dominant phytoplankton, the diatoms, into main players of marine planktonic food webs and the carbon cycle (3). Diatoms require dissolved silica [as orthosilicic acid, H_4SiO_4], which they precipitate from seawater, to form their silica (amorphous hydrated Si) frustules (4) making coastal upwelling areas also a major Si sink (5).

The prolific diatom-dominated blooms that respond to episodic inputs of nutrients are dominated by chain-forming marine species of the genus *Chaetoceros* Ehrenberg (6). Their great capacity for C export to the sediments has been shown by the observation that maximum fluxes of *Chaetoceros* coincide with intervals of increased nutrient availability in most coastal upwelling regions (California (7); Humboldt (8); Iberia-Canary (9, 10, 11, 12); Benguela (13, 14); Somalia-Oman (15, 16). Although only a

minor percentage (1–4%) of the initial diatom population gets preserved in the sediments (e.g. (12, 17, 18), the positive relationship between abundance of diatom frustules and content of organic carbon in sediments beneath major upwelling systems (*Iberia-Canary system* (19, 20); *the Benguela System* (21); *the Peru-Humboldt system* (22), *the N California system* (23) suggests that estimates of sedimentary diatom abundance (#valves/g) (SDA) represent a good marker for C export production at coastal upwelling regions. In support of this relationship, time series of organic carbon content and diatom abundance from Atlantic coastal upwelling sites indicate concomitant variations of the two productivity proxies (e.g. 24, 25). Conversely, other sequences from the NW and SW African margins show contradictory results (e.g. 26, 27,28). A time series located off Oregon (29) also shows disagreement between carbon and diatom-based estimates of primary productivity. In this record, high abundances of small diatoms, which dominate highly productive ecosystems, co-occur with low concentrations of total organic carbon (TOC) in the sediments while higher carbon burial rates seem to be associated with the accumulation of large diatoms typical of unproductive environments.

That the physical and chemical processes as well as the biological response in coastal upwelling have a non-linear and complex relation has long been recognized (30). Furthermore, intra- and inter-regional variability is known to be extensive across space and through time demanding dynamical and fine-scale biological modeling to faithfully understand those complex interactions. Here we analyze an extensive dataset of sedimentary diatom abundance (SDA; 703 sites) and organic carbon content (TOC; 200 sites) in concert with mean annual values of net primary production, upwelling index, and seawater nutrient concentrations extracted from long time-series and global climatologies to assess the main factors controlling SDA. Our study relies on two main arguments, 1) it is possible to make generalizations about the functioning of coastal upwelling ecosystems (30), and 2) the sediments retain the imprint of the different processes that, on average, determine the physical, chemical and biological properties of coastal upwelling ecosystems

MATERIALS AND METHODS

The used data set comprises 703 sediment samples recovered from the five most important coastal upwelling areas of the modern ocean, by different institutions and sampling processes (box-, multi- and in some cases piston- coring devices since the 70's). For the analysis, the topmost sediment (0-1 or -2 cm) was used (Figure 1; Supplementary Information (SI Table 1). Calibration between the diatom data produced

by different researchers followed the process described by (31), and counting principles followed (32). Obtained values are given as number of valves / g of dry-sediment (#valves/g) and show a 4 orders of magnitude variability, between 10^5 and 10^9 . Considering that cell growth is exponential, and to avoid the effect of extreme values and preserve minor variability within each order of magnitude, the data is plotted as its natural log (ln).

Organic Carbon content (TOC - %w) for the Galiza, Portuguese Margin, NW Africa – Canary, SE and NE Pacific was measured following the methodology in use at the IPMA sedimentology and micropalontology laboratory. Three replicates of 2 mg subsamples of each dried and homogenized sediment sample are measured, before and after combustion, on a CHNS-932 LECO elemental analyzer. The relative precision of repeated measurements of both samples and standards was 0.03 w%.

Upwelling indices were determined accordingly to the National Oceanic and Atmospheric Administration (NOAA) procedure (33) http://las.pfeg.noaa.gov/las/doc/global_upwell.html. Geostrophic winds were calculated from the FNMOG 6-hourly pressure analysis (1° grid). Wind stress and Ekman transport were then calculated from these geostrophic winds. Finally, the Ekman transport is rotated to get the offshore component, provided that the orientation of the coast is known, and a monthly upwelling index was obtained for each site location from 1969 to 2013.

Net Primary Production (NPP) data was provided by the Oregon State University Ocean Productivity Center (<http://www.science.oregonstate.edu/ocean.productivity/>) as mean annual and seasonal values for the available 10-year dataset (2003-2013). NPP is determined by, the Vertically Generalized Production Model (VGPM) and is a function of chlorophyll, available light, and the photosynthetic efficiency (34).

The *World Ocean Atlas 2013* (WOA13) is the source for *in situ* measured phosphate, silicate, and nitrate in μM at standard depth levels and for annual, seasonal, and monthly compositing periods (35). Surface values correspond to the 10 m water depth and bottom data comprises the closest available value for each sample site water depth.

To address the long-term global relation between SDA and all the environmental variables, escaping the temporal variability (seasonal and annual) within and between regions, we used the annual mean value estimated from the number of years of available data. Regressions between SDA and each variable annual mean were calculated and the corresponding plot generated for the entire dataset as well as for the sites confined to the main upwelling zone of each system. The latitudinal boundaries for each main upwelling area were set to include seasonal upwelling regions and followed (36).

RESULTS AND DISCUSSION

a) Sedimentary Organic Carbon (TOC) and Diatom Abundance (SDA)

Our dataset allows to evaluate the relationship between SDA and TOC per geographic region and globally (200 sites; Table 1 and Figure 2). No relation exists for the Canary upwelling System (Galiza to Canaries), the Benguela and the Peru-Humboldt systems, but a positive and significant relationship was found for the California system (NW Pacific) ($R^2 = 0.98$, $p=0.01$, $n=5$). When the entire existing dataset is considered, a significant positive relation is obtained ($R^2 = 0.40$, $p=0.01$, $n=200$). These results suggest that small-scale regional conditions are likely to determine different SDA and TOC accumulation loci (e.g. 37). Diatoms give a detailed picture of the centers of maximum annual primary production generated during the upwelling season (38, 39). TOC is indicative of the mean annual production independently of the generating process. On a global scale, the covariance between SDA and TOC is likely to reflect the higher annual contribution of diatoms to total carbon export in the high-Si coastal upwelling systems.

When dealing with sediment components, however, one has to verify to which extent can sedimentary processes alter the sediment record. Both diatom and organic carbon burial success depend on the (1) sealing effect provided by the rate of contribution of other particles to the bulk sediment, that is, sediment accumulation rate (MAR) and (2) early diagenetic processes on the seafloor (40):

(1) Sealing effect: MAR is a rate that can only be calculated if knowing the age of the sediments and it is subject to errors that can be caused by faulty age models, or yet processes like sediment focusing by bottom currents. Such problems can only be circumvented through the combined use of MAR estimation from excess ^{230}Th determinations (41). For our sites, little or no ^{230}Th data is available, and dated cores are scarce and punctual, reducing the original data set to the 28 sites (SI Table 3). We used these data to investigate the possible influence of MAR variability on diatom accumulation rate (DAR) according to:

$$\text{DAR (\# valves cm}^{-2} \text{ ky}^{-1}) = \text{Diatom abundance (\#valves/g)} * \text{MAR (g cm}^{-2} \text{ ky}^{-1})$$

Where MAR ($\text{g cm}^{-2} \text{ ky}^{-1}$) is calculated multiplying the sedimentation rate (SR, cm/yr) * by the sediment dry bulk density (g/cm^3)

Sediment dry bulk density is also not available for the majority of the dated cores, but one can consider its variability between 0.7 and 2 g/cm^3 (authors laboratory data for thousands of samples). SR was determined on the basis of the two topmost published radiocarbon dates for each site (SI Table 3). Both DAR and MAR were estimated using the minimum, mean and maximum dry bulk density (SI Figure 1A, B). The results

reveal that SDA is not dependent on MAR ($R^2=0.01$), while DAR values are mainly controlled by diatom abundance ($R^2=0.90$).

When the same exercise is performed for TOC values, the data set gets reduced to 10 sites which is not representative of all 5 areas and shows no relation to either MAR ($R^2=0.18$ at $p=0.1$ and $n=10$), nor TOC accumulation rate ($R^2=0.62$ at $p=0.1$ and $n=10$).

(2) Diatom and TOC diagenetic effects at the sea floor:

Diatom regeneration on the seafloor, although influenced by factors such as pH, temperature, organic matter and metal ions associated with the frustule surface, it is dominated by the slowly kinetic rates of dissolution related to the degree of Si saturation in the medium, that is, the concentration of silicic acid in the bottom waters (e.g. 42, 43, 44).

No relation between SDA and concentration of silicic acid in deep waters was found at the regional level (SI Figure 2). Throughout the world ocean, the pathway of thermohaline deep water circulation generates inter-basin differences in the concentration of silicic acid, which increases as deep waters flow from the Atlantic Ocean to the Southern and Pacific basins (45). The comparison of bottom $[H_4SiO_4]$ to SDA at our sites displays the two expected clusters that separate the lower silicate of the Atlantic vs the higher silicate of the Pacific (Figure 3). As to the SDA (ln transformed), statistically different mean values are found for the two clusters (t test: $T= -20.481$, $p<0.001$, mean Atlantic= 5.606 ± 0.072 and mean Pacific/Indian = 6.696 ± 0.076), but a large overlap in the diatom abundance of the two clusters is also evident. These results indicate that despite the diatom losses related to sea-floor $[Si(OH)_4^-]$, the preserved sediment diatom signal carries generalized information which is more than the result of dissolution effects.

The preservation of organic matter that escapes water-column degradation and reaches the bottom is dependent on the type of organic matter, bioturbation level and mainly bottom water oxygenation (46, 47, 48). Aside from the long-standing debate regarding the kinetics of organic matter decomposition reaction to different bottom-water O_2 concentration, Canfield (1994) showed that at high rates of organic carbon deposition, typical of continental margins, differences in preservation are poorly dependent on bottom water O_2 concentrations.

b) Upwelling Intensity and SDA

In the modern subtropical ocean coastal upwelling is mostly seasonal (Spring-Summer) but in the more tropical latitudes of a few locations such as off Cape Blanc (Canary System), Walvis-bay (Benguela system), off Peru (Humboldt system) it is

perennial. Inter-annual atmospheric and oceanic variations can cause latitudinal extension and retraction in the seasonal spatial coverage of each system as well as in the offshore extension of upwelling filaments. The best-known and dramatic inter-annual variations in coastal upwelling derived primary production occurs in the Humboldt-Peru system, caused by the El Niño-Southern Oscillation (ENSO) Cycle (49, 50).

To investigate the possible effect of upwelling strength on the sediment diatom abundance, we used a 47yr annual mean of the upwelling index for each sample site. The method of (33) can generate errors for sites located within 1 degree off the coast or close to the equator. That is, the inner-shore areas, which constitute the most influenced by the coastal upwelling process, and represent a large number of our sites (519 in total – SI Figure 3). An alternative approach would be the use of local wind datasets, but problems arise from the fact that different areas have dissimilar data sets both in terms of time length as in the index calculation approach. As such, we decided to use the NOAA dataset after exclusion of the very large values. The results (SI Figure 4; Table 1) reveal that independently of using all the sites or just the main upwelling areas, the only significant relationship is for the Southern Hemispheric systems (Benguela and Humboldt – Table 1). As a whole, the physics although essential, does not appear as the primary factor determining diatom bloom size and its sediment record.

c) Primary production and SDA

On the global scale, the restricted coastal upwelling areas are always highly associated to the spatial distribution of primary production, independently of the methodological approach (51, 52). There is also evidence for a good relationship between primary production and sediment diatom abundance, at the regional level (e.g. Figs 1E and 8 in (31) and 6 in (53)). The relationship between the sediment diatom abundance data and NPP at each of this study sites is presented in figure 4A. Although the general positive relation between SDA and NPP, a significant correlation is only found for the area of the Canary system with perennial upwelling conditions (Table 1). However, a close inspection of figure 4A reveals that if data from different geographic locations is incorporated, three possible different correlation lines could be defined, reflecting a combination of intra-regional differences and inter-regional similarities in the SDA-NPP relationship. In any way, this result hampers the possibility of defining a single equation at the global level.

d) Nutrient Availability and SDA

The variables evaluated so far revealed that SDA, contrarily to what has been found at the regional level, is not solely influenced by upwelling strength or ecosystem productivity. Neither sedimentary processes seem to be a major determinant of SDA. Thus, we explored the role of nutrient availability in regulating SDA under the premise that nutrient supply ratios can select for specific phytoplankton groups (54, 55, 49).

In coastal upwelling areas the type and amount of nutrients delivered to the ocean surface depends on the upwelling intensity (discussed above) since it determines the water mass source depth. Upwelled waters are in general, central waters of sub-polar and sub-tropical origin in different mixing proportions. On a global scale, the previously mentioned inter-ocean fractionation also causes different nutrient concentrations to exist in the Atlantic and the Pacific coastal upwelling source waters. Similarly, intra-ocean circulation determines nutrient differences at the hemispheric level, in particular for silicate concentrations (40, 49, 56).

In coastal upwelling areas, diatoms dominate the biomass of phytoplankton communities. Their obligate requirement for silicic acid makes it a limiting nutrient for diatom growth (57, 58). Mesocosm experiments revealed that marine diatoms dominate phytoplankton communities when the concentration of silicic acid exceeds $2\mu\text{M}$ whenever other nutrients are in excess (59). Further analyses have shown that diatom productivity is limited by the availability of silicic acid in broad regions of the global ocean such as the equatorial Pacific (60).

To evaluate the large-scale spatial and temporal relation between surface water major nutrients content and SDA we used mean annual $[\text{NO}_3^-]$, $[\text{PO}_4^{2-}]$ and $[\text{Si}(\text{OH})_4^-]$ from the WOA13 database (Table 1, SI figure 5 and figure 4). SDA has significant positive relationships to $[\text{NO}_3^-]$ and $[\text{PO}_4^{2-}]$ on the Humboldt (0.44 and 0.52 respectively, at $p=0.1$ and $n=162$) and the Somalia-Oman systems (0.79 and 0.67 at $p=0.1$ and $n=23$), but not at the global level, as it is also clear from SI figure 5. When the data set is restricted to the main upwelling areas the positive relationship between SDA and nitrate becomes positive and significant (0.39 at $p=0.1$ and $n=400$), consistent with the effect of nitrate on diatom standing stocks.

We found a statistically significant relationship between SDA and $[\text{Si}(\text{OH})_4^-]$ for the Canary, Humboldt and Oman Systems (0.52, 0.49 and 0.74 respectively –see Table 1). The relationship was also significant for the Benguela system (0.41 at $p=0.1$ and $n=32$) when only the main upwelling areas are considered (Table 1; Figure 4). Figure 4 and SI Figure 6A represent the relation found for SDA and silicate for the main upwelling sites and the total dataset respectively, and show the same but a reduction in data scattering when only the main upwelling areas are considered (figure 4B). In detail, it reveals a steep slope near the low silicate concentrations ($\leq 2\mu\text{M}$) defined by the NE Atlantic

regions (Galiza to the Canary Islands region – 29°N). The Canary (Cape Blanc), Benguela and Humboldt systems data define an increase towards the asymptote and maximum diatom abundance established by the Somalia-Oman and California system sites, the Si-richest within the modern coastal upwelling systems. This pattern is retained when treating the Atlantic and Pacific oceans data independently (SI Fig. 6 B, C), which confirms that the inter-hemispheric difference in preservation potential is not the main cause behind the global SDA pattern.

These results led us to explore the possible link between SDA and $[\text{Si}(\text{OH})_4^-]$ in the surface waters using a theoretical framework focused on cell physiology. Our strategy assumes that the observed SDA reflects surface ocean diatom productivity and export fluxes. The concentration of silicic acid in the upwelled waters can potentially increase SDA in two ways: 1) increasing diatom productivity (and hence diatom numerical abundance) and 2) increasing the thickness and sinking rate of diatom frustules. Our model considers that the physiological response of marine diatoms to surface waters silicic acid availability represents a long-term (tens to hundreds of years) control on coastal upwelling SDA. It has been shown that diatom productivity increases with increasing silicic acid concentrations in broad regions of the ocean (60). Thus, we speculate that silicic acid concentration sets an upper limit to diatom growth rate, which is imposed by the physiological capacity of individual cells to take up and use silicic acid.

The dynamics of silicic acid uptake by diatoms has been a matter of continuous debate (61, 62), but it is traditionally parameterized by a Michaelis-Menten model, defined by two parameters, the maximum uptake rate and the half saturation constant (i.e. the concentration of nutrient at which the population reaches half of the maximum uptake rate); (63). We applied the mathematical expression used to model nutrient uptake kinetics to our SDA data at the regional, oceanic, hemispheric and global scale:

$$V = V_{\text{max}} [S] / (K_s + [S])$$

where V_{MAX} is considered to be the maximum diatom abundance value (Diat_{MAX}) defined by the best line fit (ln) to the data; $[S]$ the concentration of silicic acid; ($\text{Si}_{\text{surfMAX}}$) and K_s the half saturation constant defined as $\text{Diat}_{\text{MAX}}/2$ (Diat_S).

The results obtained are presented in SI table 2, where the parameter V represents the expected sediment diatom abundance at a given silicic acid concentration in the surface ocean waters. All 5 areas, Pacific and Indian coastal upwelling areas V takes a value in the order of 10^8 for a for silicic acid concentration $\pm 7\mu\text{M l}^{-1}$. For the Southern Hemisphere coastal upwelling systems the values were in the order of 10^7 for the same $[\text{Si}] \pm 7\mu\text{M l}^{-1}$. The parameter V in the Atlantic Ocean is one order of magnitude lower than in the Southern Hemisphere systems and two orders of magnitude lower than in the Pacific Ocean or all the 5 areas together. Similarly, a $[\text{Si}]$ yield-dose of $1\mu\text{M}$ in the Atlantic and North Hemisphere (excluding the Somalia-Oman system), suggests that in

these oceanic regions marine diatoms are outcompeted by non-siliceous phytoplankton in agreement with observations in mesocosm experiments (59).

In conclusion, our results indicate that SDA is not dependent on sedimentation rate nor is it just a function of the bottom water silicate concentration. On decadal to centennial time scales, nitrate and silicic acid concentrations in surface waters contribute to define global SDA pattern. However, the ability of marine diatoms to take up silicic acid sets an upper limit to SDA that strongly influences the potential of coastal upwelling areas for C sequestration.

Acknowledgments

This study was supported by the following projects: CUPEX (PDCT/MAR/56963/2004) and Diatbio (PTDC/AAG-GLO/3737/2012). The authors thank Cremilde Monteiro and Apolónia Inês by their laboratory support, L. Dewitt for her help with the upwelling index calculation, and CCC for their review of the initial version of this work.

LIST OF TABLES AND FIGURES

Table 1 – Pearson correlation between the total Sediment Diatom Abundance data set (SDA as $\ln(\# \text{ valves/g})$ and ecological parameters (UPindex – 47 year annual mean upwelling index; NPP – 10 year annual mean Net Primary Production from VGPM; N – WOA13 [NO_3^-]; P – WOA13 [PO_4^{2-}]; Si_{surf} – WOA13 [$\text{Si}(\text{OH})_4^-$]; Si_b – WOA09 [$\text{Si}(\text{OH})_4^-$] at site depth; TOC – Sedimentary organic carbon content as W%) for each upwelling area and all the 5 areas. Upwelling considers the data points located under the main upwelling areas. Bold numbers indicate the highest significant correlations. Factors followed by (-) indicate negative factors, for which the signal of the correlation value has to be multiplied by -1.

Figure 1 – Geographic distribution of the total data set sites considered in this study. Map in WGS84 and Mercator projection. Different colors represented different upwelling systems.

Figure 2 – Relationship between total marine diatom abundance $\ln(\# \text{ valves/g})$ and total organic carbon content (W%) for the Canary (Galiza to Canary), Humboldt (SE Pacific) and California systems (NE Pacific).

Figure 3 - Relationship between total marine diatom abundance \ln (# valves /g) and bottom water $[\text{Si}(\text{OH})_4^-]$ in μM from WOA 2009 database. Color scheme as in Figure 1.

Figure 4 - Relationship between total marine diatom abundance \ln (# valves /g) to: A. NPP generated from SeaWiFS chlorophyll distributions according to the Vertically Generalized Production Model (VGPM) (34) for sites located on main upwelling areas; B. surface water $[\text{Si}(\text{OH})_4^-]$ in μM , from WOA 2013 database. Sites located on main upwelling areas. Color scheme as in Figure 1.

Supplementary Information

SI Table 1 - ID, site geographic location (latitude, longitude), and diatom abundance found for the sediment samples from each specific region. Included is also the reference to the laboratory methods used in each case.

SI Table 2 - The Michaelis-Menten hyperbolic relationship parameters defined from the long-term record of sediment diatom abundance (SDA) in the various upwelling systems separately as well as combined by ocean, hemisphere and as a whole; $V_{\text{max}} - \text{Diat}_{\text{MAX}}$; $[\text{S}] - \text{Si}_{\text{surfMAX}}$; $K_s - \text{Diat}_S = \text{Diat}_{\text{MAX}}/2$; $[\text{S}] - \text{Si}_{\text{surfS}}$.

SI Table 3 - Site geographic location (latitude, longitude), water depth, sedimentation rate (SR) and published AMS ^{14}C dates author.

SI Figure 1 - Relationship between total marine diatom abundance \ln (# valves /g) and Marine DAR \ln (# valves $\text{cm}^{-2} \text{yr}^{-1}$).

SI Figure 2 - Comparison of mean annual $[\text{Si}(\text{OH})_4^-]$ (WOA09) and SDA along the Peru-Humboldt System

SI Figure 3 - Geographic distribution of the samples complying with the 1-mile distance to the coast (shaded area).

SI Figure 4 - Relationship between total marine diatom abundance \ln (# valves /g) and a 47yr mean annual geostrophic Ekman transport determined upwelling index, for the total dataset. Different colors represented different upwelling systems.

SI Figure 5 – Relationship between total marine diatom abundance \ln (# valves /g) and surface water $[\text{NO}_3^-]$ and $[\text{PO}_4^{2-}]$ in μM from WOA 2013 database. Different colors represented different upwelling systems.

SI Figure 6 - - Relationship between total marine diatom abundance \ln (# valves /g) and surface water $[\text{Si}(\text{OH})_4^-]$ in μM , from WOA 2013 database; A. Total dataset locations, B. Atlantic Ocean, C. Pacific Ocean. Color scheme as in Figure 1.

REFERENCES

1. Barber RT & Smith RL (1984) Coastal Upwelling Ecosystems. *Academic Press*:31-68.
2. Hill EA, *et al.* (1998) Eastern Ocean Boundaries Coastal Segment (E). *The Sea*, eds Robinson AR & Brink KH (John Wiley & Sons, Inc., New York), Vol 11, pp 29-67.
3. Field C, Behrenfeld M, Randerson JT, & Falkowski P (1998) Primary Production of the Biosphere: Integrating Terrestrial and Oceanic Components. *Science* 281:237-240.
4. Lewin J & Guillard RRL (1963) DIATOMS. 17:373-414.
5. Tréguer PJ & De La Rocha CL (2013) The World Ocean Silica Cycle. *Annu. Rev. Mar. Sci.*:5:5.1–5.25.
6. Estrada M & Blasco D (1985) Phytoplankton assemblages in coastal upwelling areas. *Simposio Internacional sobre las areas de afloramiento mas importantes del oeste Africano. (Cabo Blanco y Benguela)*, eds Bas C, Margalef R, & Rubies P (Instituto de Investigaciones Pesqueras), pp 379-402.
7. Sancetta C (1995) Diatoms in the Gulf of California: Seasonal flux patterns and the sediment record for the last 15,000 years. *Paleoceanography* 10(1):67-84.
8. Romero O, Hebbeln D, & Wefer G (2001) Temporal and spatial variability in export production in the SE Pacific Ocean, evidence from siliceous plankton fluxes and surface sediment assemblages. *Deep-Sea Research* 48:2673-2697.
9. Wefer G & G. F (1993) Seasonal Patterns of Vertical Flux in Equatorial and Coastal Upwelling Areas of the Eastern Atlantic. *Deep-Sea Research*.
10. Treppke U, Lange C, & Wefer G (1996) Vertical fluxes of diatoms and silicoflagellates in the eastern equatorial Atlantic, and their contribution to the sedimentary record. *Mar. Microp.* 28:73-96.
11. Lange CB, Treppke UF, & Fischer G (1994) Seasonal diatom fluxes in the Guinea Basin and their relationships to trade winds, hydrography and upwelling events. *Deep-Sea Research I* 41, N° 5/6:859-878.
12. Abrantes F, *et al.* (2002) Fluxes of micro-organisms along a productivity gradient in the Canary Islands region (29 N): implications for paleoreconstructions. *Deep-Sea Research II* 49:3599-3629.
13. Treppke U, *et al.* (1996) Diatom and silicoflagellate fluxes at the Walvis Ridge: An environment influenced by coastal upwelling in the Benguela system. *Journal of Marine Research* 54:991-1016.
14. Romero O, *et al.* (2002) Seasonal productivity dynamics in the pelagic central Benguela System inferred from the flux of carbonate and silicate organisms. *J. Mar. Syst* 37:259-278.
15. Koning E, *et al.* (2001) Selective preservation of upwelling-indicating diatoms in sediments off Somalia, NW Indian Ocean. *Deep Sea Research Part I: Oceanographic Research Papers* 48:2473:2495.
16. Nair RR, *et al.* (1989) Increased particle flux to the deep ocean related to monsoons. *Nature* 338:749-751.

17. Sancetta C (1992) Comparison of phytoplankton in sediment trap series and surface sediments along productivity gradient. *Paleoceanography* 7(2):183-194.
18. Takahashi K, Honjo S, & Tabata S (1989) Siliceous phytoplankton flux: interannual variability and response to hydrographic changes in the northeastern Pacific. *Aspects of Climate Variability in the Pacific and Western Americas.*, ed Peterson D (Amer. Geophysical Union), Vol Monograph 55, pp 151-160.
19. Abrantes F (1988) Diatom assemblages as upwelling indicators in surface sediments in Portugal. *Marine Geology* 85:15-39.
20. Nave S, Freitas P, & Abrantes F (2001) Coastal upwelling in the Canary Island region: spatial variability reflected by the surface sediment diatom record. *Marine Micropaleontology* 42:1-23.
21. Schuette G & Schrader H (1981) Diatom Taphocoenoses in the Coastal Upwelling Area off South West Africa. (Elsevier Scientific Publishing Company, Amsterdam), pp 131-155.
22. Abrantes F (2004) The Modern SE Pacific Diatom Record. What can we learn for further Paleoclimatic and Paleoceanographic Reconstructions. *AGU Fall Conference*, ed AGU.
23. Lopes C, Mix AC, & Abrantes F (2006) Diatoms in northeast Pacific surface sediments as paleoceanographic proxies. *Marine Micropaleontology* 60(1):45-65.
24. Abrantes F (2000) 200 ka Diatom Records from Atlantic Upwelling sites Reveal Maximum Productivity during LGM and a Shift in Phytoplankton Community Structure at 185 ka. *Earth Planetary Science Letters* 176:7-16.
25. Muller PJ & Suess E (1979) Productivity, sedimentation rate, and sedimentary organic matter in the oceans - I. Organic carbon preservation. *Deep-Sea Research* 26A:1347 pp.
26. Martinez P, et al. (1999) Upwelling intensity and ocean productivity changes off Cape Blanc (northwest Africa) during the last 70,000 years: geochemical and micropalaeontologica. *Marine Geology* 158:57-74.
27. Caulet J-P, Vénec-Peyré M-T, Vergnaud-Grazzini C, & Nigrini C (1992) Variations of South Somalian upwelling during the last 160 ka: radiolarian and foraminifera records in core MD 85674. *Upwelling Systems: Evolution Since the Early Miocene*, eds Summerhayes C, Prell W, & Emeis K (The Geological Society, London), p 379:389.
28. Heinze P & Wefer G (1992) The history of coastal upwelling off Peru (11°S, ODP Leg 112, Site 680B) over the past 650000 years. *Upwelling Systems: Evolution Since the Early Miocene*, eds Summerhayes C, Prell W, & Emeis K (The Geological Society, London), pp 451-462.
29. Lopes C, Kucera M, & Mix A (2014) Climate change decouples oceanic primary and export productivity and organic carbon burial. *PNAS*.
30. Barber R & Smith R (1981) Coastal Upwelling Ecosystems. *Analysis of Marine Ecosystems*, ed Longhurst AR (Academic Press, New York), pp 31-68.
31. Abrantes F, I. G, Lopes C, & Castro M (2005) Quantitative diatom analyses—a faster cleaning procedure. *Deep Sea Research Part I: Oceanographic Research Papers* 52:189:198.
32. Schrader H & Gersonde R (1978) Diatoms and Silicoflagellates. *Utrecht Micropaleontological Bulletins* 17:129-176.
33. Bakun A (1973) Coastal upwelling indices, west coast of North America, 1946-1971, 403 NOAA Technical Report NMFS SSRF-671, 103. in *NOAA Technical Report*
34. Behrenfeld M & Falkowski P (1997) Photosynthetic rates derived from satellite-based chlorophyll concentration. *Limnology and Oceanography* 42:1-20.
35. Garcia HE, et al. (2014) World Ocean Atlas 2013, Volume 4: Dissolved Inorganic Nutrients (phosphate, nitrate, silicate). S. Levitus. in *NOAA Atlas NESDIS 76* (A. Mishonov Technical Ed, NODC), p 25.
36. Rykaczewski R, et al. (2015) Poleward displacement of coastal upwelling favorable winds in the ocean's eastern boundary currents through the 21st century. *Geophys. Res. Lett.*
37. Reimers C & Suess E (1983) Late Quaternary fluctuations in the cycling of organic

- matter off central Peru: A proto-kerogen record. *Coastal Upwelling Its Sediment Record*, ed Suess JTaE (Plenum-Press).
38. Abrantes F & Moita T (1999) Water Column and Recent Sediment Data on Diatoms and Coccolithophorids, off Portugal, Confirm Sediment Record as a Memory of Upwelling Events. *Oceanologica Acta* 22:319-336.
 39. Nelson D, Tréguer P, Brzezinski M, Leynaert A, & Quéguiner B (1995) Production and dissolution of biogenic silica in the ocean: Revised global estimates, comparison with regional data and relationship to biogenic sedimentation. *Global Biogeochemical Cycle* 9(3):359-372.
 40. Broecker WS & Peng TH (1982) Tracers in the sea. *Tracers in the sea*, ed Broecker WS (Eldigio Press, New York).
 41. Lyle M, et al. (2014) Sediment size fractionation and focusing in the equatorial Pacific: Effect on ²³⁰Th normalization and paleoflux measurements. *Paleoceanography* 29.
 42. Hurd DC & Takahashi K (1982) On the Estimation of Minimum Mechanical Loss During an in situ Biogenic Silica Dissolution Experiment. (Elsevier Scientific Publishing Company, Amsterdam), pp 441-447.
 43. Van Cappellen P, Dixit S, & van Beusekom J (2002) Biogenic silica dissolution in the oceans: Reconciling experimental and field-based dissolution rates. *Global Geochemical Cycles* 16(4).
 44. Van Bennekom AJ & Berger GW (1984) Hydrography and silica budget of the Angola Basin. *Netherlands Journal of Sea Research* 17:149-200.
 45. Rageneau O, Tréguer P, Anderson R, Brzezinski M, & DeMaster DJ (2000) A review of the Si cycle in the modern ocean recent progress and missing gaps in the application of biogenic opal pump. *Global Biogeochem. Cycles* 20(GB4Si02).
 46. Canfield DE (1994) Factors influencing organic carbon preservation in marine sediments. *Chemical Geology* 114(3-4):315-329.
 47. Emerson S (1985) Organic Carbon Preservation in Marine Sediments. *The Carbon Cycle and Atmospheric CO: Natural Variations Archean to Present*, eds Sundquist ET & Broecker WS (American Geophysical Union, Washington, D. C.), doi: 10.1029/GM032p0078 Ed.
 48. Zonneveld K, et al. (2010) Selective preservation of organic matter in marine environments; processes and impact on the sedimentary record. *Biogosciences* 7:483-511.
 49. Barber R & Kogelschatz J (1990) Nutrients and Productivity during the 1982/83 El Niño. *Global Ecological Consequences of the 1982-1983 El Nino-Southern Oscillation*, ed Glyn PNew York), pp 21-53.
 50. Philander SGH (1990) *El Niño, La Niña, and the Southern Oscillation* (Academic Press, San Diego).
 51. Berger WH (1989) Global Maps of Ocean Productivity. *Productivity of the Ocean: Present and Past.*, Lifr Sciences Research Reports, eds Berger WH, Smetacek VS, & Wefer G (John Wiley & Sons, New York), 1 Ed Vol 1, pp 429-455.
 52. Gregg W & Conkright M (2008) Global Seasonal Climatologies of Ocean Chlorophyll: Blending In situ and Satellite Data for the CZCS Era (NOAA, National Oceanographic Data Center (NODC)).
 53. Lopes C, Mix A, & Abrantes F (2005) Diatom Transfer Functions for Sea Surface Temperature and Productivity in Upwelling Regimes: A Canonical Correspondence Analysis Approach. *EGU General Assembly*, (European Geosciences Union), pp EUG05-A-01079.
 54. Raymont J (1980) *Plankton and Productivity in the Oceans* (Pergamon Press, Oxford) 2nd Ed.
 55. Platt T, et al. (1992) Nutrient control of phytoplankton photosynthesis in the Western North Atlantic. pp 229-231.
 56. Sarmiento JL, Gruber N, Brzezinski M, & Dunne JP (2003) High-latitude controls of thermocline nutrients and low latitude biological productivity. *Nature* 427:56:60.
 57. Brzezinski M & Nelson D (1996) Chronic substrate limitation of silicic acid uptake rates in the western Sargasso Sea. *Deep Sea Research Part II: Oceanographic*

Research Papers 43:437-453.

58. Lima D, Lam PJ, & Doney SC (2014) Dynamics of particulate organic carbon flux in a global ocean model. *Biogeosciences* 11:1177–1198.
59. Egge JK & Aksnes D (1992) Silicate as regulating nutrient in phytoplankton competition. *Marine Ecology Progress Series* 83:281-289.
60. Dugdale R & Wilkerson FP (1998) Silicate regulation of new production in the equatorial Pacific upwelling. *Nature* 391(6664):270.
61. Thamatrakoln K & Hildebrand M (2008) Silicon Uptake in Diatoms Revisited: A Model for Saturable and Nonsaturable Uptake Kinetics and the Role of Silicon Transporters. *Plant physiology* 146(3):1397-1407.
62. Dugdale RC (1967) Nutrient limitation in the sea: dynamics, identification, and significance. *Limnology and Oceanography* 12:685-695.
63. Del Amo Y & MA. B (1999) The chemical form of dissolved Si taken up by marine diatoms. *Journal of Phycology* 35:1162–1170.

Table 1

Areas	n Upidex		n Upidex Tup		n NPP		n NPP Tup		n Sil b		n Sil b Tup		n Si surf		n Si surf Tup		n P		n N		n P Tup		n N Tup		n TOC (W ⁹)	
	43yr ann mean		43yr ann mean		10yr ann mean		10yr ann mean		(site water depth)		(site water depth)		(10 m)		(10 m)										(sedimen)	
Galiza / Portuguese-Canary System	11	0.09	-	-	11	-0.19	-	-	10	-0.24	-	-	10	-0.24	-	-	10	0.24	0.24	-	-	-	-	11	0.51	
Portuguese Margin / Portuguese-Canary System	119	0.14	-	-	111	0.22	-	-	61	0.16	-	-	61	-0.21	-	-	73	-0.35	-0.24	-	-	-	-	85	0.08	
NW Africa / Portuguese-Canary System	37	0.00	-	-	37	-0.03	-	-	34	-0.27	-	-	34	0.12	-	-	34	0.23	-0.10	-	-	-	-	30	0.31	
NW Africa / Canary System	21	-0.01	-	-	50	0.10	-	-	35	0.19	-	-	50	0.52	-	-	50	0.08	0.16	-	-	-	-	na	na	
SW Africa / Benguela System	61	0.34	28	0.35	62	0.24	38	0.64	62	-0.05	32	-0.27	52	-0.08	32	0.41	62	0.25	0.33	32	0.30	0.23	-	na	na	
SE Pacific / Humboldt System	176	0.41	116	0.41	207	0.18	166	0.15	162	0.07	116	0.07	162	0.49	116	0.51	162	0.52	0.44	116	0.58	-0.21	43	0.15		
NE Pacific / California System	62	-0.12	20	-0.16	63	-0.05	19	0.14	37	0.03	21	0.14	37	0.03	21	-0.05	43	0.08	0.06	21	0.04	0.09	5	0.98		
Oman / Indian Monsson	26	-0.16	-	-	33	0.36	-	-	23	-0.03	-	-	23	0.74	-	-	23	0.67	0.79	-	-	-	-	na	na	
TOTAL	513	0.04	378	0.13	573	0.09	463	0.09	422	0.15	338	0.19	429	0.27	353	0.31	400	0.04	0.06	303	0.16	0.39	174	0.43		

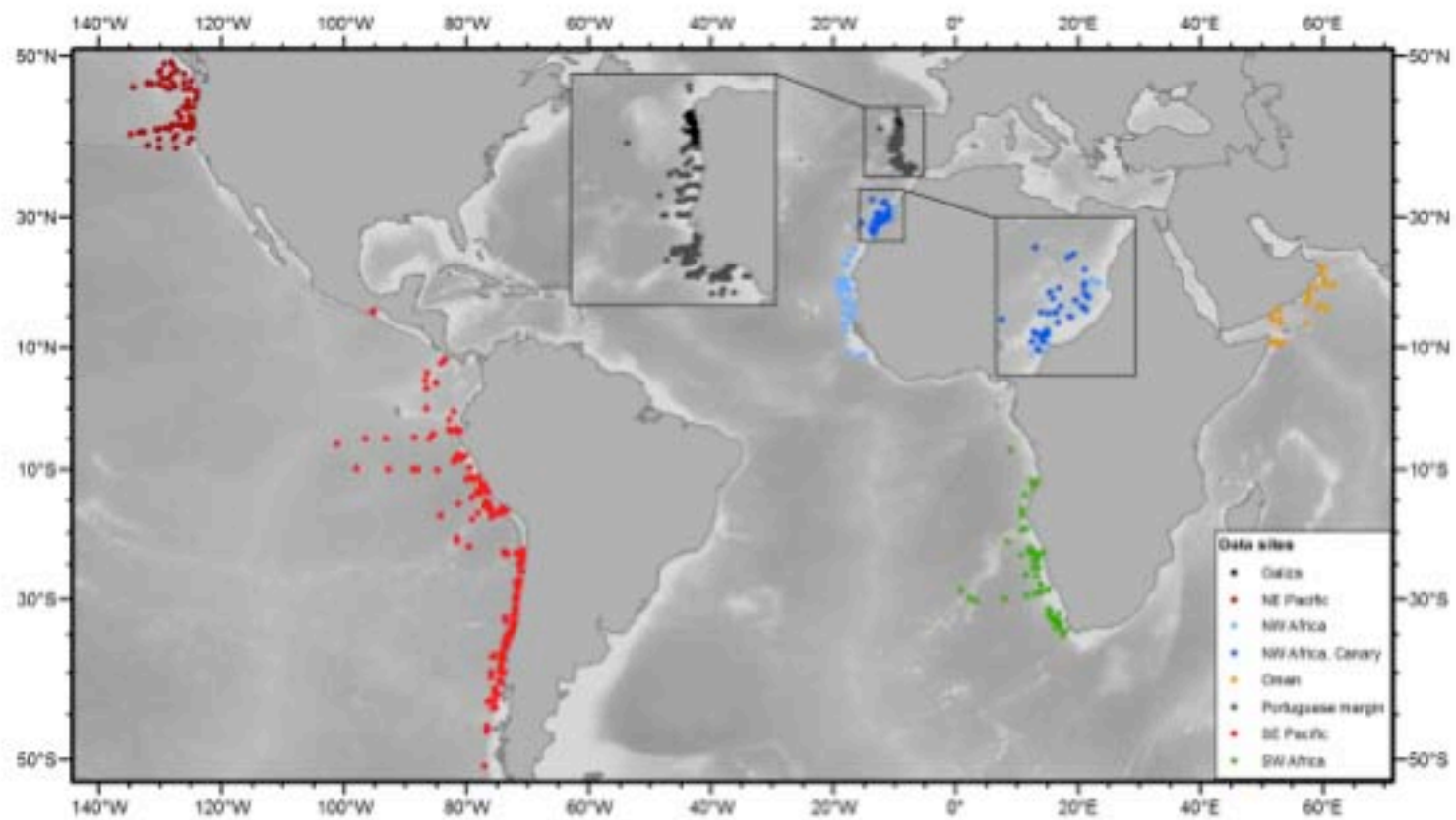


Figure 1

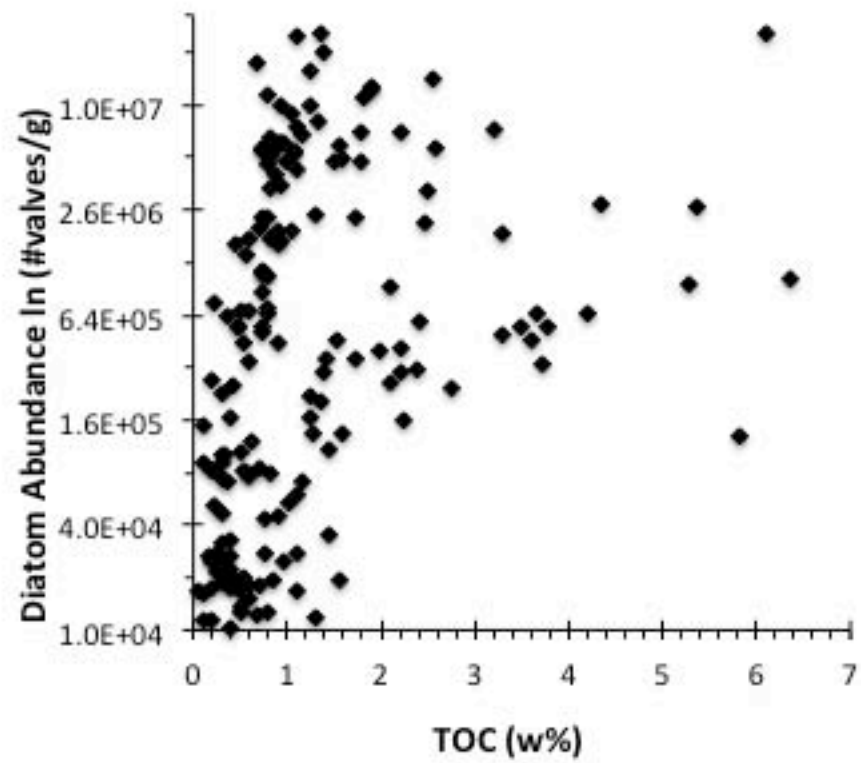


Figure 2

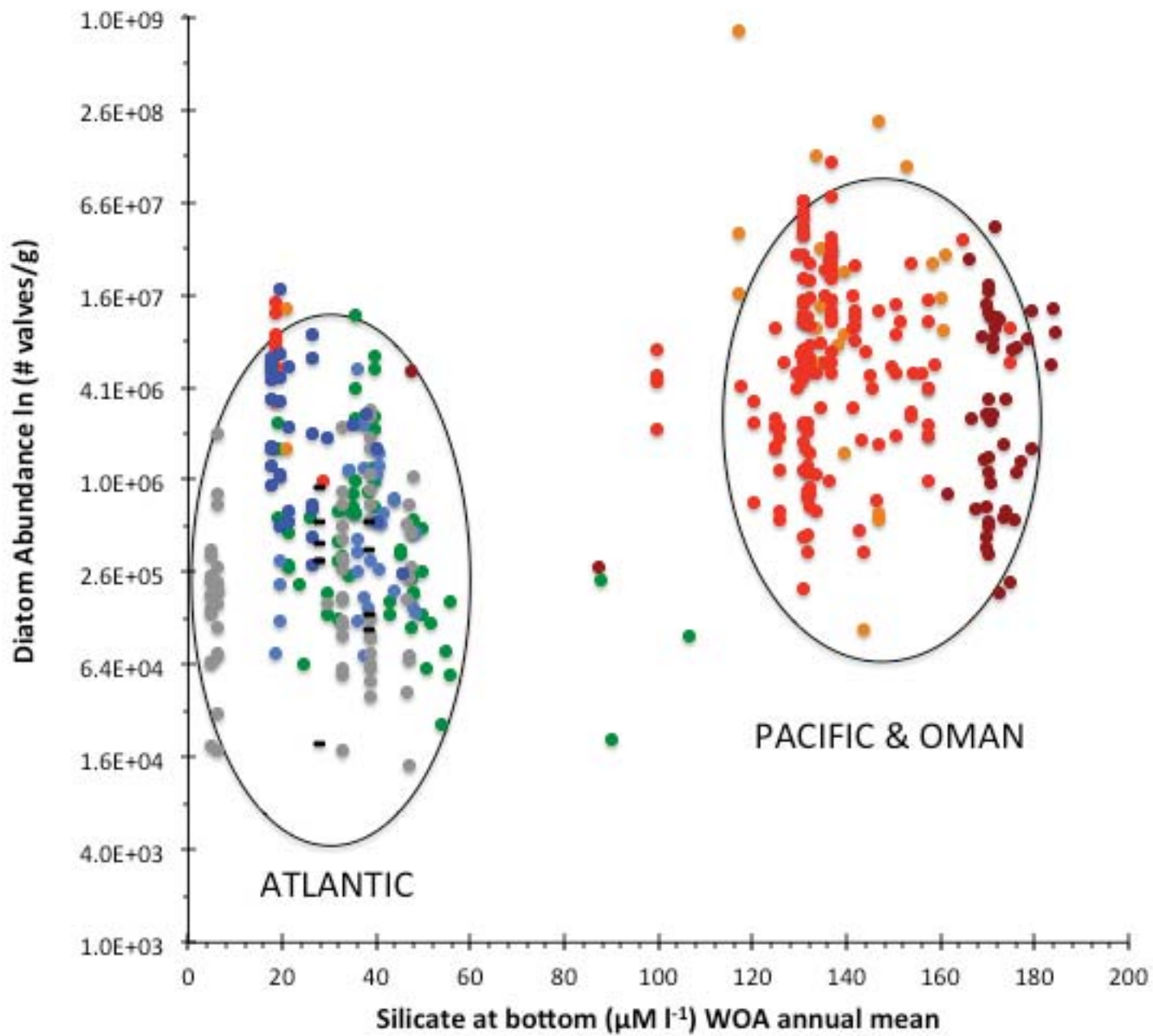


Figure 3

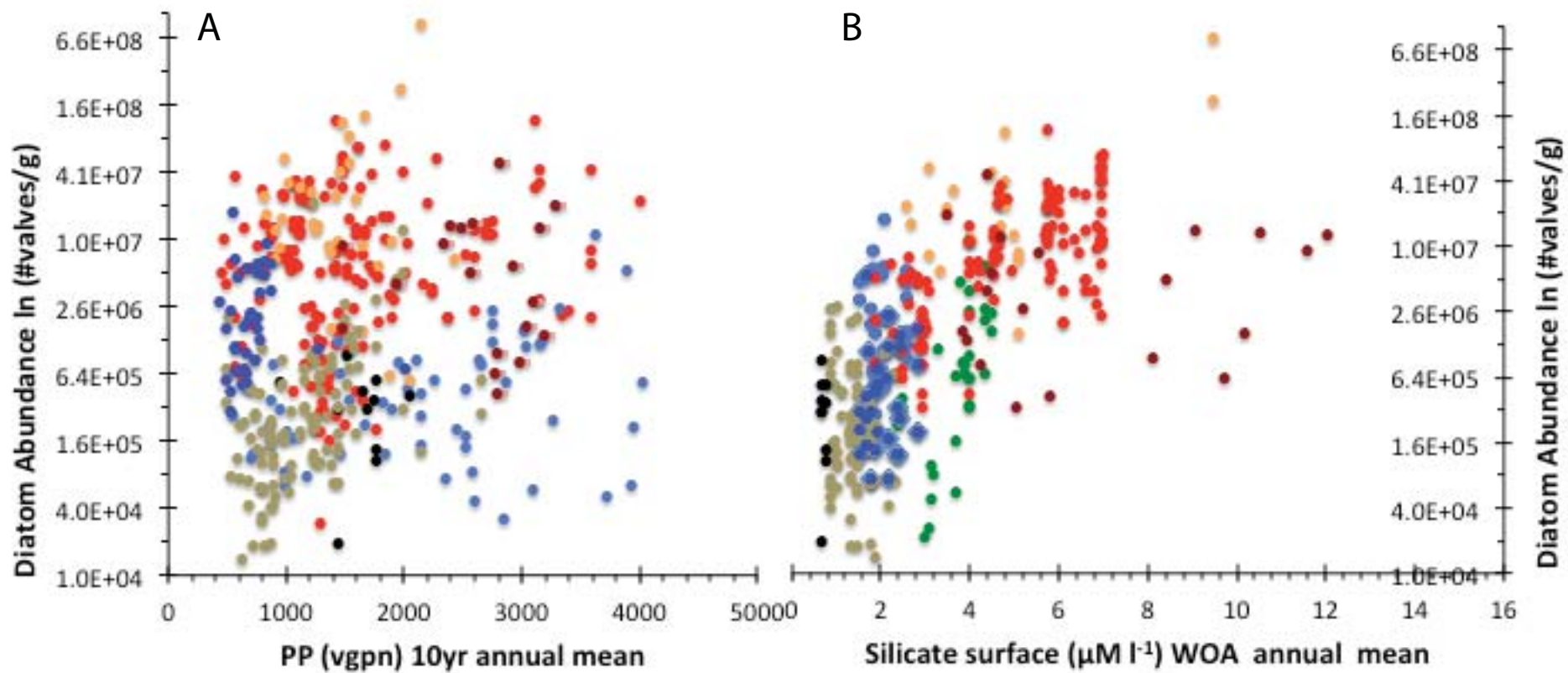


Figure 4

SI Table 1

Location	Station	Latitude (S -; N +)	Longitude (W -; E +)	Depth (m)	SDA (#valves/g)	Author / Counting Method
Galiza	11039-1	41.55	-9.08	99	553027	Fatima Abrantes/Cristina Lopes
Galiza	11043-1	41.55	-9.00	84	134954	Fatima Abrantes/Cristina Lopes
Galiza	11041-1	41.63	-9.01	93	107778	Fatima Abrantes/Cristina Lopes
Galiza	11042-1	41.72	-9.02	95	362745	Fatima Abrantes/Cristina Lopes
Galiza	11002-1	42.17	-8.99	111	450669	Fatima Abrantes/Cristina Lopes
Galiza	11003-2	42.17	-9.04	129	913266	Fatima Abrantes/Cristina Lopes
Galiza	11033-1	42.17	-9.56	1873	541586	Fatima Abrantes/Cristina Lopes
Galiza	11010-1	42.42	-9.11	118	398120	Fatima Abrantes/Cristina Lopes
Galiza	11017-1	42.52	-9.24	120	305255	Fatima Abrantes/Cristina Lopes
Galiza	11013-1	42.71	-9.35	130	300657	Fatima Abrantes/Cristina Lopes
Galiza	11014-1	42.71	-9.46	153	19631	Fatima Abrantes/Cristina Lopes
PT Margin	116	41.58	-8.87	40	4493330	Fatima Abrantes
PT Margin	120	41.58	-9.02	85	2920000	Fatima Abrantes
PT Margin	123	41.59	-9.16	100	1100000	Fatima Abrantes
PT Margin	124	41.58	-9.19	105	130430	Fatima Abrantes
PT Margin	165	40.81	-9.20	140	885710	Fatima Abrantes
PT Margin	167	40.81	-9.08	95	700000	Fatima Abrantes
PT Margin	168	40.81	-9.02	85	1625000	Fatima Abrantes
PT Margin	170	40.81	-8.93	50	12000000	Fatima Abrantes
PT Margin	172	40.81	-8.82	35	5000000	Fatima Abrantes
PT Margin	174	40.81	-8.73	10	300000	Fatima Abrantes
PT Margin	215	39.72	-9.07	20	414290	Fatima Abrantes
PT Margin	218	39.72	-9.18	70	900000	Fatima Abrantes
PT Margin	219	39.72	-9.23	100	764710	Fatima Abrantes
PT Margin	221	39.72	-9.33	130	94510	Fatima Abrantes
PT Margin	224	39.72	-9.43	130	178130	Fatima Abrantes
PT Margin	226	39.72	-9.50	145	194440	Fatima Abrantes
PT Margin	242	39.09	-9.45	30	1050000	Fatima Abrantes
PT Margin	244	39.08	-9.53	52	1200000	Fatima Abrantes
PT Margin	246	39.08	-9.58	62	300000	Fatima Abrantes
PT Margin	248	39.08	-9.67	94	452170	Fatima Abrantes
PT Margin	249	39.08	-9.70	94	600000	Fatima Abrantes
PT Margin	252	39.08	-9.77	116	593850	Fatima Abrantes
PT Margin	254	39.08	-9.83	144	100000	Fatima Abrantes
PT Margin	256	39.09	-9.94	154	285710	Fatima Abrantes
PT Margin	273	37.14	-7.50	80	11100000	Fatima Abrantes
PT Margin	276	37.07	-7.50	47	92860	Fatima Abrantes
PT Margin	277	37.04	-7.50	74	166330	Fatima Abrantes
PT Margin	278	37.00	-7.50	95	180950	Fatima Abrantes
PT Margin	280	36.95	-7.50	180	74470	Fatima Abrantes
PT Margin	282	36.91	-7.50	405	160710	Fatima Abrantes
PT Margin	287	36.91	-7.80	235	275790	Fatima Abrantes
PT Margin	317	36.84	-8.17	95	66670	Fatima Abrantes
PT Margin	326	36.89	-8.87	110	183330	Fatima Abrantes
PT Margin	338	37.06	-8.67	33	175000	Fatima Abrantes
PT Margin	339	37.05	-8.67	36	909090	Fatima Abrantes
PT Margin	341	37.03	-8.67	38	2500000	Fatima Abrantes
PT Margin	343	37.00	-8.67	63	127270	Fatima Abrantes
PT Margin	345	36.97	-8.67	80	66670	Fatima Abrantes
PT Margin	347	36.93	-8.67	98	184620	Fatima Abrantes
PT Margin	349	36.90	-8.67	105	136840	Fatima Abrantes
PT Margin	351	36.88	-8.67	110	325000	Fatima Abrantes
PT Margin	369	36.92	-9.05	93	700000	Fatima Abrantes
PT Margin	386	37.58	-8.87	95	209090	Fatima Abrantes
PT Margin	387	37.58	-8.88	110	250000	Fatima Abrantes
PT Margin	388	37.58	-8.90	118	1025000	Fatima Abrantes
PT Margin	389	37.59	-8.92	129	794440	Fatima Abrantes

Location	Station	Latitude (S-; N +)	Longitude (W -; E +)	Depht (m)	SDA (#valves/g)	Author / Counting Method
PT Margin	393	37.59	-8.98	160	100000	Fatima Abrantes
PT Margin	395	37.58	-9.02	190	312500	Fatima Abrantes
PT Margin	397	37.58	-9.05	245	313330	Fatima Abrantes
PT Margin	415	37.92	-8.94	105	261900	Fatima Abrantes
PT Margin	426	38.08	-8.90	112	252630	Fatima Abrantes
PT Margin	445	37.81	-9.20	450	851060	Fatima Abrantes
PT Margin	451	38.22	-8.97	140	113330	Fatima Abrantes
PT Margin	453	38.23	-8.91	120	200000	Fatima Abrantes
PT Margin	455	38.24	-8.87	105	211110	Fatima Abrantes
PT Margin	457	38.25	-8.83	60	1000000	Fatima Abrantes
PT Margin	458	38.25	-8.81	35	21500000	Fatima Abrantes
PT Margin	698	40.19	-9.53	158	50000	Fatima Abrantes
PT Margin	700	40.19	-9.40	135	75000	Fatima Abrantes
PT Margin	702	40.21	-9.19	100	566670	Fatima Abrantes
PT Margin	703	40.20	-9.11	85	2687500	Fatima Abrantes
PT Margin	704	40.20	-9.07	65	1950000	Fatima Abrantes
PT Margin	706	40.19	-8.99	45	500000	Fatima Abrantes
PT Margin	708	40.19	-8.93	18	1500000	Fatima Abrantes
PT Margin	709	40.14	-8.89	10	740000	Fatima Abrantes
PT Margin	1316	41.74	-12.41	5035	42000	Fatima Abrantes
PT Margin	1318	42.24	-9.67	2080	161000	Fatima Abrantes
PT Margin	1324	40.95	-9.57	2010	40000	Fatima Abrantes
PT Margin	1325	40.72	-10.03	1880	274000	Fatima Abrantes
PT Margin	1327	40.57	-10.34	3380	468000	Fatima Abrantes
PT Margin	1331	39.91	-9.78	1045	57000	Fatima Abrantes
PT Margin	1335	37.37	-10.50	4950	73000	Fatima Abrantes
PT Margin	1340	37.29	-9.33	900	55000	Fatima Abrantes
PT Margin	1343	36.83	-9.34	787	69820	Fatima Abrantes
PT Margin	1361	36.74	-7.81	645	18000	Fatima Abrantes
PT Margin	1363	36.85	-7.82	618	198000	Fatima Abrantes
PT Margin	1365	36.90	-7.82	300	192000	Fatima Abrantes
PT Margin	1366	36.77	-8.01	735	19000	Fatima Abrantes
PT Margin	1368	36.69	-7.93	725	31000	Fatima Abrantes
PT Margin	1369	36.63	-7.88	745	113000	Fatima Abrantes
PT Margin	1937	36.75	-6.57	16	550000	Fatima Abrantes
PT Margin	1938	36.74	-6.54	17	285085	Fatima Abrantes
PT Margin	1939	36.74	-6.70	52	1538596	Fatima Abrantes
PT Margin	1940	37.10	-7.21	18	125512	Fatima Abrantes
PT Margin	2351	37.53	-9.33	820	173000	Fatima Abrantes
PT Margin	2353	37.84	-9.85	2331	270000	Fatima Abrantes
PT Margin	2354	37.56	-9.27	636	514000	Fatima Abrantes
PT Margin	2356	37.58	-9.42	986	174000	Fatima Abrantes
PT Margin	2360	37.86	-9.55	1300	18000	Fatima Abrantes
PT Margin	2362	37.46	-9.60	1699	125000	Fatima Abrantes
PT Margin	2393	38.32	-9.10	420	121000	Fatima Abrantes
PT Margin	2861	37.84	-9.71	2010	428000	Fatima Abrantes
PT Margin	2863	37.81	-9.37	900	98000	Fatima Abrantes
PT Margin	2865	37.82	-9.08	267	704000	Fatima Abrantes
PT Margin	2970	37.32	-9.52	1271	61000	Fatima Abrantes
PT Margin	2979	37.64	-9.93	2200	2260000	Fatima Abrantes
PT Margin	2981	37.61	-10.05	2315	232000	Fatima Abrantes
PT Margin	2985	39.63	-9.76	1620	42000	Fatima Abrantes
PT Margin	2987	39.62	-9.84	1824	191000	Fatima Abrantes
PT Margin	2989	39.63	-9.93	1940	34000	Fatima Abrantes
PT Margin	2999	40.56	-9.65	2247	64000	Fatima Abrantes
PT Margin	3008	41.43	-9.73	2371	102000	Fatima Abrantes
PT Margin	3010	41.49	-9.72	2160	60000	Fatima Abrantes
PT Margin	3019	41.63	-9.48	1800	97000	Fatima Abrantes
PT Margin	3082	37.80	-10.17	3146	14000	Fatima Abrantes

Location	Station	Latitude (S-; N +)	Longitude (W -; E +)	Depht (m)	SDA (#valves/g)	Author / Counting Method
PT Margin	3083	36.03	-7.78	1205	713000	Fatima Abrantes
PT Margin	3085	36.11	-7.22	800	76000	Fatima Abrantes
PT Margin	3087	36.24	-7.73	967	2050000	Fatima Abrantes
PT Margin	3089	36.78	-7.71	580	831000	Fatima Abrantes
PT Margin	3090	36.65	-7.41	532	223000	Fatima Abrantes
PT Margin	3093	36.71	-8.26	667	151000	Fatima Abrantes
PT Margin	3094	36.71	-8.26	668	244000	Fatima Abrantes
PT Margin	3095	36.74	-8.26	728	219000	Fatima Abrantes
PT Margin	3096	36.05	-8.23	1918	356000	Fatima Abrantes
PT Margin	3098	37.82	-9.50	1082	116000	Fatima Abrantes
PT Margin	3100	39.04	-10.68	1977	532802	Fatima Abrantes
PT Margin	3101	39.07	-10.54	1605	169000	Fatima Abrantes
PT Margin	3103	43.79	-9.44	2170	1060000	Fatima Abrantes
PT Margin	3104	40.58	-9.86	2465	133000	Fatima Abrantes / Silvia Nave
NW Africa - Canary	VH4025-	27.75	-13.49	496	686772	Fatima Abrantes / Silvia Nave
NW Africa - Canary	VH4026-	27.81	-13.54	990	1087122	Fatima Abrantes / Silvia Nave
NW Africa - Canary	VH4040-	28.19	-13.34	1000	1268140	Fatima Abrantes / Silvia Nave
NW Africa - Canary	M4233-2	28.47	-13.33	1303	5178178	Fatima Abrantes / Silvia Nave
NW Africa - Canary	M4234-1	28.47	-13.23	1360	5487038	Fatima Abrantes / Silvia Nave
NW Africa - Canary	M4235-1	28.47	-13.18	1244	1632151	Fatima Abrantes / Silvia Nave
NW Africa - Canary	M4236-2	28.47	-13.10	1030	6050821	Fatima Abrantes / Silvia Nave
NW Africa - Canary	M4237-1	28.47	-13.02	800	3482951	Fatima Abrantes / Silvia Nave
NW Africa - Canary	M4238-2	28.47	-13.64	1185	1661434	Fatima Abrantes / Silvia Nave
NW Africa - Canary	M4239-1	28.47	-13.18	881	6242978	Fatima Abrantes / Silvia Nave
NW Africa - Canary	VH4057-	28.58	-13.74	1000	4645826	Fatima Abrantes / Silvia Nave
NW Africa - Canary	VH4038-	28.68	-13.04	695	950789	Fatima Abrantes / Silvia Nave
NW Africa - Canary	M4223-1	29.02	-12.47	777	517112	Fatima Abrantes / Silvia Nave
NW Africa - Canary	M4301-1	29.17	-15.45	3610	2746540	Fatima Abrantes / Silvia Nave
NW Africa - Canary	M4225-3	29.28	-11.78	1281	540176	Fatima Abrantes / Silvia Nave
NW Africa - Canary	M4226-1	29.32	-11.83	1400	5568547	Fatima Abrantes / Silvia Nave
NW Africa - Canary	M4228-1	29.47	-12.99	1633	17833071	Fatima Abrantes / Silvia Nave
NW Africa - Canary	M4229-1	29.48	-12.65	1426	6733488	Fatima Abrantes / Silvia Nave
NW Africa - Canary	M4230-1	29.48	-12.60	1316	1122999	Fatima Abrantes / Silvia Nave
NW Africa - Canary	M4232-1	29.48	-13.39	1161	2297229	Fatima Abrantes / Silvia Nave
NW Africa - Canary	M4212-3	29.60	-10.95	1256	856867	Fatima Abrantes / Silvia Nave
NW Africa - Canary	M4213-1	29.70	-11.08	1547	2275041	Fatima Abrantes / Silvia Nave
NW Africa - Canary	M4227-1	29.77	-12.34	1826	1078491	Fatima Abrantes / Silvia Nave
NW Africa - Canary	M4214-3	29.78	-11.20	1788	642290	Fatima Abrantes / Silvia Nave
NW Africa - Canary	M4215-1	30.04	-11.55	2106	708014	Fatima Abrantes / Silvia Nave
NW Africa - Canary	M4211-1	30.19	-10.82	1773	4769057	Fatima Abrantes / Silvia Nave
NW Africa - Canary	M4210-2	30.30	-10.98	1959	3364111	Fatima Abrantes / Silvia Nave
NW Africa - Canary	M4209-1	30.36	-11.08	2150	2025008	Fatima Abrantes / Silvia Nave
NW Africa - Canary	M4217-5	30.42	-12.91	2506	288665	Fatima Abrantes / Silvia Nave
NW Africa - Canary	M4217-1	30.44	-12.90	2504	439913	Fatima Abrantes / Silvia Nave
NW Africa - Canary	M4216-1	30.63	-12.40	2324	669993	Fatima Abrantes / Silvia Nave
NW Africa - Canary	M4208-1	30.71	-11.08	2724	6292611	Fatima Abrantes / Silvia Nave
NW Africa - Canary	M4207-1	30.86	-11.07	2123	9153764	Fatima Abrantes / Silvia Nave
NW Africa - Canary	M4206-2	31.50	-11.02	1855	1930436	Fatima Abrantes / Silvia Nave
NW Africa - Canary	M4204-1	32.02	-11.95	3213	546056	Fatima Abrantes / Silvia Nave
NW Africa - Canary	M4205-1	32.18	-11.65	3272	1621139	Fatima Abrantes / Silvia Nave
NW Africa - Canary	M4202-1	32.48	-13.66	4289	249967	Fatima Abrantes / Silvia Nave
NW Africa	9533-3	8.93	-14.91	384	493529	Oscar Romero
NW Africa	9532-1	8.95	-14.89	317	363546	Oscar Romero
NW Africa	9528-1	9.17	-17.66	3057	179205	Oscar Romero
NW Africa	9529-1	9.35	-17.37	1229	64123	Oscar Romero
NW Africa	9525-5	12.64	-17.88	2652	85089	Oscar Romero
NW Africa	9516-4	13.67	-18.42	3504	240580	Oscar Romero
NW Africa	9517-5	13.72	-18.19	3125	794436	Oscar Romero
NW Africa	9519-6	13.81	-17.68	1479	262116	Oscar Romero

Location	Station	Latitude (S-; N +)	Longitude (W -; E +)	Depth (m)	SDA (#valves/g)	Author / Counting Method
NW Africa	9520-4	13.83	-17.59	1102	110618	Oscar Romero
NW Africa	9515-2	15.27	-17.04	102	84738	Oscar Romero
NW Africa	9513-4	15.32	-17.29	494	855850	Oscar Romero
NW Africa	9512-4	15.34	-17.37	793	366059	Oscar Romero
NW Africa	9510-3	15.42	-17.65	1566	1198919	Oscar Romero
NW Africa	9508-4	15.49	-17.95	2384	58149	Oscar Romero
NW Africa	9506-3	15.61	-18.35	2956	32135	Oscar Romero
NW Africa	9502-5	16.28	-16.67	63	561561	Oscar Romero
NW Africa	9501-4	16.80	-16.73	323	472326	Oscar Romero
NW Africa	8521-3	16.96	-17.82	2688	148790	Oscar Romero
NW Africa	8519-1	16.97	-17.83	2676	260725	Oscar Romero
NW Africa	8520-3	16.98	-17.83	2689	421255	Oscar Romero
NW Africa	8522-3	17.25	-18.37	3097	301288	Oscar Romero
NW Africa	8524-3	17.84	-17.26	2178	756544	Oscar Romero
NW Africa	8501-1	18.50	-18.76	2995	72651	Oscar Romero
NW Africa	7932-2	19.00	-17.28	1964	533361	Oscar Romero
NW Africa	7928-3	19.10	-17.05	1350	1190160	Oscar Romero
NW Africa	8502-4	19.22	-18.93	2956	173630	Oscar Romero
NW Africa	8503-1	19.25	-18.98	3194	468176	Oscar Romero
NW Africa	8509-3	19.45	-18.09	2584	1772421	Oscar Romero
NW Africa	8507-1	19.47	-18.10	2414	2348036	Oscar Romero
NW Africa	8508-1	19.47	-18.10	2453	1236148	Oscar Romero
NW Africa	8506-1	19.71	-17.72	1828	2394918	Oscar Romero
NW Africa	8517-1	19.72	-17.42	1480	5433314	Oscar Romero
NW Africa	7927-1	19.94	-19.15	3116	204317	Oscar Romero
NW Africa	7926-1	20.21	-18.45	2500	1125540	Oscar Romero
NW Africa	8631-8	20.47	-17.82	500	225388	Oscar Romero
NW Africa	8505-1	20.52	-19.16	3205	835033	Oscar Romero
NW Africa	8504-1	20.58	-19.17	3246	138931	Oscar Romero
NW Africa	7922-3	20.74	-18.18	1516	1244447	Oscar Romero
NW Africa	7920-3	20.75	-18.58	2278	1521938	Oscar Romero
NW Africa	8630-8	20.82	-17.97	1327	536706	Oscar Romero
NW Africa	8625-1	23.08	-17.50	1294	627886	Oscar Romero
NW Africa	8626-2	23.14	-17.84	2255	168658	Oscar Romero
NW Africa	8627-2	23.20	-18.17	2668	11007011	Oscar Romero
NW Africa	8533-1	24.28	-17.53	2184	213818	Oscar Romero
NW Africa	8531-1	24.39	-17.15	1896	197159	Oscar Romero
NW Africa	8532-1	24.43	-17.19	2125	781682	Oscar Romero
NW Africa	8620-2	25.36	-16.54	1871	343571	Oscar Romero
NW Africa	8614-2	27.54	-13.85	1440	121884	Oscar Romero
NW Africa	8608-4	28.00	-13.00	974	47051	Oscar Romero
NW Africa	8601-1	30.85	-10.27	924	121886	Oscar Romero
NW Africa	8607-2	30.91	-10.36	1068	122225	Oscar Romero
NW Africa	8604-3	30.96	-10.52	883	75094	Oscar Romero
NW Africa	8606-2	31.00	-10.74	1222	301663	Oscar Romero
SW Africa	3603-1	-35.12	17.53	2851	118384	Oscar Romero
SW Africa	3602-1	-34.79	17.76	1885	259966	Oscar Romero
SW Africa	3601-1	-34.64	17.86	945	135702	Oscar Romero
SW Africa	8301-5	-34.46	17.42	1941	500930	Oscar Romero
SW Africa	8303-5	-34.16	16.48	3447	60104	Oscar Romero
SW Africa	8307-5	-33.83	16.50	2668	187108	Oscar Romero
SW Africa	8306-1	-33.74	16.84	1923	187108	Oscar Romero
SW Africa	8305-1	-33.48	17.18	712	63976	Oscar Romero
SW Africa	8311-1	-33.37	16.31	2565	561820	Oscar Romero
SW Africa	8310-1	-32.91	16.38	1995	189914	Oscar Romero
SW Africa	8315-5	-32.89	15.70	2995	239562	Oscar Romero
SW Africa	8316-1	-32.74	15.73	2666	247104	Oscar Romero
SW Africa	8317-1	-32.33	15.16	2926	113807	Oscar Romero
SW Africa	8318-1	-32.15	16.81	280	135952	Oscar Romero

Location	Station	Latitude (S -; N +)	Longitude (W -; E +)	Depth (m)	SDA (#valves/g)	Author / Counting Method
SW Africa	3604-4	-31.79	15.50	1510	167200	Oscar Romero
SW Africa	3605-1	-31.45	15.30	1373	135966	Oscar Romero
SW Africa	1726-1	-30.27	3.26	1006	48093	Oscar Romero
SW Africa	1724-2	-29.97	8.09	5084	681314	Oscar Romero
SW Africa	1728-3	-29.84	2.41	2887	80933	Oscar Romero
SW Africa	1722-3	-29.45	11.75	3074	229803	Oscar Romero
SW Africa	1721-4	-29.18	13.09	3079	165591	Oscar Romero
SW Africa	1721-5	-29.17	13.09	3045	55308	Oscar Romero
SW Africa	1720-4	-29.00	13.84	2004	78031	Oscar Romero
SW Africa	1719-4	-28.93	14.17	1023	586006	Oscar Romero
SW Africa	1729-1	-28.89	1.00	4401	26235	Oscar Romero
SW Africa	1718-1	-28.71	15.21	167	159316	Oscar Romero
SW Africa	1716-3	-27.96	14.00	1479	215858	Oscar Romero
SW Africa	8469-3	-26.75	13.37	1480	1224274	Oscar Romero
SW Africa	1715-1	-26.47	11.64	4095	99395	Oscar Romero
SW Africa	8470-1	-25.54	12.85	2470	864912	Oscar Romero
SW Africa	8455-1	-25.50	13.18	1503	6625476	Oscar Romero
SW Africa	8451-1	-25.47	13.35	1028	2682445	Oscar Romero
SW Africa	8450-1	-25.47	13.60	506	683630	Oscar Romero
SW Africa	8449-1	-25.47	13.55	605	2196515	Oscar Romero
SW Africa	8448-2	-25.47	13.44	806	5439455	Oscar Romero
SW Africa	3606-2	-25.47	13.08	1793	1037118	Oscar Romero
SW Africa	8452-1	-25.42	13.68	388	1002853	Oscar Romero
SW Africa	8422-1	-24.45	12.70	1997	679293	Oscar Romero
SW Africa	8424-3	-24.42	12.92	1519	840347	Oscar Romero
SW Africa	8421-4	-24.38	13.05	1205	1658009	Oscar Romero
SW Africa	8419-2	-24.35	13.22	834	2439292	Oscar Romero
SW Africa	8403-1	-24.25	13.60	320	582183	Oscar Romero
SW Africa	1709-3	-23.59	10.76	3837	21165	Oscar Romero
SW Africa	8402-1	-23.47	13.80	164	272799	Oscar Romero
SW Africa	1711-6	-23.32	12.37	1975	356236	Oscar Romero
SW Africa	1712-1	-23.25	12.81	1004	333519	Oscar Romero
SW Africa	1713-6	-23.22	13.02	597	288092	Oscar Romero
SW Africa	1713-5	-23.22	13.01	600	464713	Oscar Romero
SW Africa	8481-2	-23.00	12.95	597	12046737	Oscar Romero
SW Africa	8482-2	-23.00	12.88	704	629823	Oscar Romero
SW Africa	8483-2	-23.00	12.84	805	4030917	Oscar Romero
SW Africa	8484-3	-23.00	12.77	950	630850	Oscar Romero
SW Africa	8498-2	-23.00	12.57	1442	2601175	Oscar Romero
SW Africa	8499-1	-23.00	12.33	2080	1003050	Oscar Romero
SW Africa	8404-2	-22.99	14.35	44	16617662	Oscar Romero
SW Africa	84100-2	-22.99	11.99	2725	645670	Oscar Romero
SW Africa	3608-1	-22.36	12.20	1972	244227	Oscar Romero
SW Africa	4911-2	-21.38	8.48	1950	1971976	Oscar Romero
SW Africa	1707-2	-19.70	10.66	1234	662217	Oscar Romero
SW Africa	1705-2	-19.50	11.38	647	642981	Oscar Romero
SW Africa	1704-1	-19.41	11.62	399	128544	Oscar Romero
SW Africa	1703-3	-17.45	11.02	1771	4349743	Oscar Romero
SW Africa	2308-1	-16.73	11.04	2114	1192097	Oscar Romero
SW Africa	2309-1	-16.58	10.84	2675	1174060	Oscar Romero
SW Africa	2307-1	-14.23	11.52	2892	326075	Oscar Romero
SW Africa	4918-3	-12.84	12.70	1338	412883	Oscar Romero
SW Africa	2304-1	-12.02	12.45	2003	307894	Oscar Romero
SW Africa	2305-1	-11.94	13.25	897	975593	Oscar Romero
SW Africa	4914-5	-6.93	9.00	3971	4744349	Oscar Romero
Oman	BX325	10.68	53.55	1540	6686482	Oscar Romero
Oman	BX915	10.69	53.52	590	12013777	Jolanda VanIperen
Oman	BX902	10.78	51.58	891	1524079	Jolanda VanIperen
Oman	BX903	10.78	51.66	620	8933594	Jolanda VanIperen

Location	Station	Latitude (S-; N +)	Longitude (W -; E +)	Depth (m)	SDA (#valves/g)	Author / Counting Method
Oman	BX908	10.78	52.92	2680	15575505	Jolanda VanIperen
Oman	BX904	10.79	51.77	3395	9679788	Jolanda VanIperen
Oman	BX907	10.80	52.25	3580	29936902	Jolanda VanIperen
Oman	BX906	10.81	52.13	3540	26650353	Jolanda VanIperen
Oman	BX905	10.92	51.94	788	12259262	Jolanda VanIperen
Oman	BX929	13.71	53.24	2780	13169613	Jolanda VanIperen
Oman	CD14	13.85	57.37	788	16661992	Abrantes F.
Oman	BX923	14.51	51.68	3684	9047572	Jolanda VanIperen
Oman	BX924	14.73	51.60	2700	7764511	Jolanda VanIperen
Oman	BX925	14.78	51.52	440	1646541	Jolanda VanIperen
Oman	BX917	15.91	53.03	815	23132113	Jolanda VanIperen
Oman	BX919	16.01	52.74	3484	612195	Jolanda VanIperen
Oman	BX921	16.07	52.61	1893	562733	Jolanda VanIperen
Oman	RC62	16.15	60.67	1532	24105368	Fatima Abrantes
Oman	BX307	16.19	52.39	3997	109509	Jolanda VanIperen
Oman	RC58	16.37	59.18	1030	54757548	Fatima Abrantes
Oman	RC61	16.66	59.86	455	8432956	Fatima Abrantes
Oman	CD11	17.28	57.43	1118	41239003	Fatima Abrantes
Oman	RC9	17.77	57.58	459	24617068	Fatima Abrantes
Oman	RC23	17.99	57.59	2225	113231285	Fatima Abrantes
Oman	RC12	18.02	57.61	1500	85995624	Fatima Abrantes
Oman	RC14	18.25	57.66	4040	130028004	Fatima Abrantes
Oman	CD18	19.33	58.23	2484	851574636	Fatima Abrantes
Oman	CD23	19.71	58.98	50	220742817	Fatima Abrantes
Oman	CD30	19.92	61.70	2807	33009709	Fatima Abrantes
Oman	CD28	19.98	60.62	2020	13891006	Fatima Abrantes
Oman	CD27	20.73	60.17	1194	49334377	Fatima Abrantes
Oman	CD25	21.75	59.74	789	6846910	Fatima Abrantes
Oman	CD33	22.67	60.15	3572	5977125	Fatima Abrantes
Oman	CD34	22.68	59.75	4065	9884317	Fatima Abrantes
SE Pacific	ME005A-7	15.71	-95.29	577	26447244	Fatima Abrantes
SE Pacific	ME005A-4	15.65	-95.28	725	2638454	Fatima Abrantes
SE Pacific	ME005A-8	15.58	-95.28	1079	2801136	Fatima Abrantes
SE Pacific	ME005A-41	7.86	-83.61	1370	1877637	Fatima Abrantes
SE Pacific	ME005A-38	7.32	-84.11	1003	485045	Fatima Abrantes
SE Pacific	ME005A-14	5.85	-86.45	2045	5486565	Fatima Abrantes
SE Pacific	ME005A-15	4.61	-86.70	904	348198	Fatima Abrantes
SE Pacific	ME005A-35	4.12	-85.01	3404	2324558	Fatima Abrantes
SE Pacific	ME005A-20	3.21	-86.49	2675	5760036	Fatima Abrantes
SE Pacific	ME005A-21	0.02	-86.46	2942	4996622	Fatima Abrantes
SE Pacific	ME005A-29	-0.51	-82.00	1343	11151190	Fatima Abrantes
SE Pacific	ME005A-25	-1.85	-82.79	2203	4849662	Fatima Abrantes
SE Pacific	RR9702A-83	-13.17	-77.26	1419	2312773	Fatima Abrantes
SE Pacific	RR9702A-80	-13.48	-76.89	448	2122896	Fatima Abrantes
SE Pacific	RR9702A-82	-13.70	-76.71	264	2358852	Fatima Abrantes
SE Pacific	RR9702A-68	-16.01	-76.38	3228	8192285	Fatima Abrantes
SE Pacific	RR9702A-66	-16.13	-77.10	2575	7067483	Fatima Abrantes
SE Pacific	RR9702A-77	-16.13	-76.98	2588	12808046	Fatima Abrantes
SE Pacific	RR9702A-74	-16.24	-76.24	3476	25409360	Fatima Abrantes
SE Pacific	RR9702A-72	-16.51	-76.19	3782	10177277	Fatima Abrantes
SE Pacific	RR9702A-70	-16.73	-76.01	4124	11696323	Fatima Abrantes
SE Pacific	RR9702A-64	-17.04	-78.11	2930	1740341	Fatima Abrantes
SE Pacific	RR9702A-62	-18.09	-79.04	2937	750653	Fatima Abrantes
SE Pacific	GeoB7106-1	-22.80	-70.61	1351	9210000	Oscar Romero
SE Pacific	GeoB7108-3	-22.84	-70.58	1006	3430000	Oscar Romero
SE Pacific	GeoB7103-3	-22.87	-70.54	889	3720000	Oscar Romero
SE Pacific	RR9702A-52	-23.19	-73.35	3418	1094374	Fatima Abrantes
SE Pacific	RR9702A-50	-23.61	-73.61	3396	639460	Fatima Abrantes
SE Pacific	GeoB7114-1	-24.00	-70.83	1395	7800000	Oscar Romero

Location	Station	Latitude (S-; N +)	Longitude (W -; E +)	Depth (m)	SDA (#valves/g)	Author / Counting Method
SE Pacific	GeoB7115-1	-24.00	-70.60	523	1010000	Oscar Romero
SE Pacific	GeoB7112-1	-24.03	-70.82	2508	5820000	Oscar Romero
SE Pacific	GeoB7116-1	-26.00	-71.00	1996	189000	Oscar Romero
SE Pacific	GeoB7118-1	-26.00	-70.81	460	224000	Oscar Romero
SE Pacific	GeoB7119-1	-26.00	-70.87	954	28600	Oscar Romero
SE Pacific	GeoB7121-1	-26.00	-70.90	1442	296000	Oscar Romero
SE Pacific	GeoB7122-2	-26.00	-70.84	673	612000	Oscar Romero
SE Pacific	GeoB7123-1	-27.29	-71.05	557	2130000	Oscar Romero
SE Pacific	GeoB3374-1	-27.47	-71.17	1352	780000	Oscar Romero
SE Pacific	GeoB3376-2	-27.47	-71.36	2437	5410000	Oscar Romero
SE Pacific	GeoB3373-1	-27.50	-71.21	1580	860000	Oscar Romero
SE Pacific	GeoB7127-1	-28.38	-71.47	1462	603000	Oscar Romero
SE Pacific	GeoB7131-1	-28.38	-71.50	1650	161000	Oscar Romero
SE Pacific	GeoB7129-1	-28.42	-71.33	476	262000	Oscar Romero
SE Pacific	GeoB7130-1	-28.42	-71.61	2080	485000	Oscar Romero
SE Pacific	GeoB7133-1	-29.38	-71.64	635	367000	Oscar Romero
SE Pacific	GeoB7135-1	-29.67	-71.68	1432	666000	Oscar Romero
SE Pacific	GeoB7134-1	-29.72	-71.77	1888	466000	Oscar Romero
SE Pacific	GeoB7138-1	-30.13	-71.87	2733	2060000	Oscar Romero
SE Pacific	GeoB7137-2	-30.17	-71.73	1199	1530000	Oscar Romero
SE Pacific	GeoB7144-1	-31.16	-71.97	1961	1240000	Oscar Romero
SE Pacific	GeoB7142-2	-31.18	-71.75	481	5680000	Oscar Romero
SE Pacific	GeoB7148-1	-31.98	-71.93	2289	543000	Oscar Romero
SE Pacific	GeoB7150-1	-32.28	-71.95	1591	293000	Oscar Romero
SE Pacific	GeoB3365-1	-32.29	-72.27	2450	1650000	Oscar Romero
SE Pacific	RR9702A-48	-32.59	-73.65	3920	7097646	Fatima Abrantes
SE Pacific	GeoB3303-1	-33.21	-72.18	1983	5310000	Oscar Romero
SE Pacific	RR9702A-46	-33.28	-73.53	3852	5906238	Fatima Abrantes
SE Pacific	GeoB3311-2	-33.61	-72.05	471	200000	Oscar Romero
SE Pacific	GeoB7152-1	-33.80	-72.11	420	4670000	Oscar Romero
SE Pacific	GeoB7153-1	-33.80	-72.16	863	1810000	Oscar Romero
SE Pacific	GeoB7154-2	-33.80	-72.28	1385	1190000	Oscar Romero
SE Pacific	GeoB7155-1	-34.58	-72.89	2746	4450000	Oscar Romero
SE Pacific	GeoB7156-1	-34.58	-72.51	1247	7280000	Oscar Romero
SE Pacific	GeoB3355-4	-35.22	-73.12	1511	11100000	Oscar Romero
SE Pacific	GeoB3359-1	-35.22	-72.81	680	5140000	Oscar Romero
SE Pacific	GeoB3349-4	-35.25	-73.42	2471	15400000	Oscar Romero
SE Pacific	GeoB3357-1	-35.28	-73.22	2103	11200000	Oscar Romero
SE Pacific	RR9702A-44	-35.76	-73.01	172	5864949	Fatima Abrantes
SE Pacific	GeoB7157-1	-35.78	-73.59	2107	7210000	Oscar Romero
SE Pacific	GeoB7158-1	-35.78	-73.48	1563	2410000	Oscar Romero
SE Pacific	GeoB7159-1	-35.78	-73.23	506	441000	Oscar Romero
SE Pacific	RR9702A-39	-36.17	-73.57	510	12575403	Fatima Abrantes
SE Pacific	RR9702A-42	-36.17	-73.68	1028	14594435	Fatima Abrantes
SE Pacific	RR9702A-34	-36.53	-73.45	133	7447093	Fatima Abrantes
SE Pacific	RR9702A-31	-37.67	-75.43	3946	6809122	Fatima Abrantes
SE Pacific	RR9702A-29	-37.85	-75.75	4051	4433453	Fatima Abrantes
SE Pacific	RR9702A-25	-39.89	-75.89	4087	5586473	Fatima Abrantes
SE Pacific	RR9702A-20	-39.97	-74.47	1055	2427707	Fatima Abrantes
SE Pacific	RR9702A-22	-40.01	-74.12	430	4860771	Fatima Abrantes
SE Pacific	RR9702A-27	-40.48	-75.92	3850	7746575	Fatima Abrantes
SE Pacific	RR9702A-24	-41.30	-74.32	246	3304091	Fatima Abrantes
SE Pacific	RR9702A-12	-43.42	-76.25	3523	20258218	Fatima Abrantes
SE Pacific	RR9702A-14	-43.54	-76.48	3471	10263603	Fatima Abrantes
SE Pacific	RR9702A-10	-46.32	-76.54	2879	15854627	Fatima Abrantes
SE Pacific	RR9702A-8	-46.35	-76.67	3014	26110971	Fatima Abrantes
SE Pacific	RR9702A-6	-46.88	-76.60	3298	6259130	Fatima Abrantes
SE Pacific	RR9702A-4	-47.00	-76.62	3354	5392114	Fatima Abrantes
SE Pacific	RR9702A-1	-50.65	-76.96	3964	4120569	Fatima Abrantes

Location	Station	Latitude (S-; N +)	Longitude (W -; E +)	Depth (m)	SDA (#valves/g)	Author / Counting Method
SE Pacific	Y73-6-86	-70.97	-24.97	2925	8000000	Gretchen Schuette
SE Pacific	W7706-24	-71.15	-23.32	5107	8000000	Gretchen Schuette
SE Pacific	W7706-21	-71.81	-23.25	4400	3000000	Gretchen Schuette
SE Pacific	W7706-20	-73.75	-23.03	3717	5000000	Gretchen Schuette
SE Pacific	W7706-11	-73.89	-16.29	645	4000000	Gretchen Schuette
SE Pacific	Y71-6-22	-74.06	-16.81	5301	119000000	Gretchen Schuette
SE Pacific	Y73-7-95	-74.23	-16.42	2720	39000000	Gretchen Schuette
SE Pacific	Y71-6-17	-74.33	-16.89	6485	23000000	Gretchen Schuette
SE Pacific	Y71-6-16	-74.35	-16.91	6761	23000000	Gretchen Schuette
SE Pacific	Y71-6-20	-74.35	-16.97	7293	11000000	Gretchen Schuette
SE Pacific	Y71-6-15	-74.36	-16.93	7406	12000000	Gretchen Schuette
SE Pacific	Y71-6-18	-74.36	-16.95	7280	13000000	Gretchen Schuette
SE Pacific	Y71-6-21	-74.36	-16.85	6505	25000000	Gretchen Schuette
SE Pacific	Y71-6-19	-74.41	-17.05	5791	32000000	Gretchen Schuette
SE Pacific	Y73-7-94	-74.55	-16.85	5920	15000000	Gretchen Schuette
SE Pacific	FD75-3-14	-74.55	-16.95	6390	15000000	Gretchen Schuette
SE Pacific	Y73-6-93	-74.58	-16.77	6250	23000000	Gretchen Schuette
SE Pacific	FD75-3-15	-74.87	-17.18	4690	25000000	Gretchen Schuette
SE Pacific	Y71-6-14	-75.79	-17.67	4625	1000000	Gretchen Schuette
SE Pacific	W7706-32	-75.90	-16.29	645	6000000	Gretchen Schuette
SE Pacific	Y73-7-96	-76.30	-13.78	18	22000000	Gretchen Schuette
SE Pacific	Y71-6-24	-76.31	-15.27	4899	16000000	Gretchen Schuette
SE Pacific	W7706-33	-76.80	-15.73	2967	6000000	Gretchen Schuette
SE Pacific	W7706-36	-76.84	-13.62	370	12000000	Gretchen Schuette
SE Pacific	W7706-1	-76.85	-12.90	148	2000000	Gretchen Schuette
SE Pacific	W7706-37	-76.85	-13.63	370	32000000	Gretchen Schuette
SE Pacific	W7706-34	-76.85	-15.32	3316	24000000	Gretchen Schuette
SE Pacific	W7706-2	-76.87	-12.89	161	43000000	Gretchen Schuette
SE Pacific	W7706-35	-76.89	-13.65	592	3000000	Gretchen Schuette
SE Pacific	W7706-3	-76.96	-12.97	304	6000000	Gretchen Schuette
SE Pacific	W7706-4	-76.97	-12.98	325	8000000	Gretchen Schuette
SE Pacific	W7706-11	-77.23	-13.15	1380	11000000	Gretchen Schuette
SE Pacific	W7706-10	-77.25	-13.15	1380	14000000	Gretchen Schuette
SE Pacific	W7706-38	-77.25	-13.20	1414	12000000	Gretchen Schuette
SE Pacific	W7706-9	-77.32	-13.02	1335	12000000	Gretchen Schuette
SE Pacific	W7706-12	-77.33	-13.22	1285	7000000	Gretchen Schuette
SE Pacific	W7706-5	-77.33	-13.50	2286	54000000	Gretchen Schuette
SE Pacific	W7706-7	-77.46	-13.27	1774	21000000	Gretchen Schuette
SE Pacific	W7706-8	-77.54	-13.14	2067	40000000	Gretchen Schuette
SE Pacific	Y71-6-6	-77.57	-13.62	3801	43000000	Gretchen Schuette
SE Pacific	W7706-13	-77.67	-13.43	3470	67000000	Gretchen Schuette
SE Pacific	Y71-6-8	-77.71	-13.75	5273	30000000	Gretchen Schuette
SE Pacific	W7706-14	-77.72	-13.46	3621	67000000	Gretchen Schuette
SE Pacific	Y71-6-9	-77.72	-13.76	5371	57000000	Gretchen Schuette
SE Pacific	Y71-6-10	-77.73	-13.76	5508	45000000	Gretchen Schuette
SE Pacific	Y71-6-11	-77.74	-13.77	5594	52000000	Gretchen Schuette
SE Pacific	Y71-6-7	-77.77	-13.76	5374	41000000	Gretchen Schuette
SE Pacific	W7706-40	-77.96	-11.26	186	29000000	Gretchen Schuette
SE Pacific	W7706-39	-77.96	-11.25	186	120000000	Gretchen Schuette
SE Pacific	Y73-7-97	-78.08	-13.95	4620	34000000	Gretchen Schuette
SE Pacific	FD75-3-16	-78.08	-13.95	4653	28000000	Gretchen Schuette
SE Pacific	W7706-41	-78.12	-11.34	411	11000000	Gretchen Schuette
SE Pacific	W7706-42	-78.12	-11.34	411	15000000	Gretchen Schuette
SE Pacific	W7706-43	-78.23	-11.41	584	2000000	Gretchen Schuette
SE Pacific	W7706-44	-78.23	-11.41	580	1000000	Gretchen Schuette
SE Pacific	W7706-45	-78.29	-11.44	810	2000000	Gretchen Schuette
SE Pacific	W7706-15	-78.31	-13.81	4581	21000000	Gretchen Schuette
SE Pacific	W7706-47	-78.43	-11.67	1500	4000000	Gretchen Schuette
SE Pacific	W7706-49	-79.10	-11.28	3970	5000000	Gretchen Schuette

Location	Station	Latitude (S -; N +)	Longitude (W -; E +)	Depth (m)	SDA (#valves/g)	Author / Counting Method
SE Pacific	Y71-6-4	-79.12	-14.61	4518	28000000	Gretchen Schuette
SE Pacific	Y71-8-58	-79.24	-11.63	6189	31000000	Gretchen Schuette
SE Pacific	Y71-8-56	-79.24	-11.64	6256	34000000	Gretchen Schuette
SE Pacific	Y71-8-55	-79.25	-11.64	6309	34000000	Gretchen Schuette
SE Pacific	W7706-50	-79.97	-11.68	4902	7000000	Gretchen Schuette
SE Pacific	W7706-57	-80.18	-7.93	192	1000000	Gretchen Schuette
SE Pacific	W7706-61	-80.43	-8.06	838	4000000	Gretchen Schuette
SE Pacific	W7706-62	-80.80	-8.22	2670	5000000	Gretchen Schuette
SE Pacific	W7706-63	-80.92	-8.28	4513	30000000	Gretchen Schuette
SE Pacific	W7706-76	-81.00	-3.58	365	2000000	Gretchen Schuette
SE Pacific	W7706-83	-81.04	-7.67	3103	71000000	Gretchen Schuette
SE Pacific	W7706-74	-81.41	-3.76	713	3000000	Gretchen Schuette
SE Pacific	W7706-73	-81.48	-3.49	2116	16000000	Gretchen Schuette
SE Pacific	W7706-76	-81.60	-8.12	5122	32000000	Gretchen Schuette
SE Pacific	W7706-72	-81.64	-3.52	3601	10000000	Gretchen Schuette
SE Pacific	W7706-64	-81.94	-8.82	4404	12000000	Gretchen Schuette
SE Pacific	W7706-71	-82.51	-3.68	3600	4000000	Gretchen Schuette
SE Pacific	W7706-70	-85.33	-4.22	3453	14000000	Gretchen Schuette
SE Pacific	W7706-69	-85.34	-4.20	3537	5000000	Gretchen Schuette
SE Pacific	W7706-84	-85.95	-5.00	4010	9000000	Gretchen Schuette
SE Pacific	W7706-68	-88.51	-4.82	3903	13000000	Gretchen Schuette
SE Pacific	W7706-30	-88.68	-10.05	4237	2000000	Gretchen Schuette
SE Pacific	W7706-33	-92.67	-10.00	4093	4000000	Gretchen Schuette
SE Pacific	W7706-87	-93.08	-5.05	3858	37000000	Gretchen Schuette
SE Pacific	W7706-88	-96.44	-5.01	3650	6000000	Gretchen Schuette
SE Pacific	W7706-35	-97.94	-9.95	4010	5000000	Gretchen Schuette
SE Pacific	W7706-89	-101.03	-5.98	3990	10000000	Gretchen Schuette
NE Pacific	W8209-19 GC	39.30	-127.40	4355	4040000	Cristina Lopes
NE Pacific	W8209B-1 GC	39.63	-132.06	4560	222000	Cristina Lopes
NE Pacific	Y73-10-100 GC	40.00	-125.30	1935	1400000	Cristina Lopes
NE Pacific	TT34-1 GC	40.52	-130.05	3287	666000	Cristina Lopes
NE Pacific	L6-85-NC 7 GC	40.53	-127.71	3195	820000	Cristina Lopes
NE Pacific	M9907-39PC	40.60	-124.80		7500000	Cristina Lopes
NE Pacific	M9907-40	40.60	-124.90		2700000	Cristina Lopes
NE Pacific	L6-85-NC 3GC	41.00	-127.30	2983	12600000	Cristina Lopes
NE Pacific	W8909A-48GC	41.30	-132.70		5810000	Cristina Lopes
NE Pacific	W8909A-57	41.60	-130.60		10100000	Cristina Lopes
NE Pacific	W8809A-51 GC	41.66	-128.35	3159	514000	Cristina Lopes
NE Pacific	EW9504-16	41.70	-124.80		11200000	Cristina Lopes
NE Pacific	W8809-11GC	41.70	-126.00	3020	19900000	Cristina Lopes
NE Pacific	W8809A-29 GC	41.80	-129.01	3288	430000	Cristina Lopes
NE Pacific	W8709A13PC	42.10	-125.80		45600000	Cristina Lopes
NE Pacific	W8909-24GC	42.10	-125.30	2790	48000000	Cristina Lopes
NE Pacific	W7905A-173	42.20	-124.90		8420000	Cristina Lopes
NE Pacific	W7905A-174G	42.20	-124.70		2490000	Cristina Lopes
NE Pacific	W8809A-19GC	42.20	-126.50	2669	2760000	Cristina Lopes
NE Pacific	W8909-31	42.20	-127.20	2800	5050000	Cristina Lopes
NE Pacific	W8809A-26 GC	42.21	-128.01	3034	337000	Cristina Lopes
NE Pacific	Y6708-25	42.29	-124.58		3470000	Cristina Lopes
NE Pacific	W89097GC	42.30	-124.90	1100	5810000	Cristina Lopes
NE Pacific	Y6708-23	42.36	-124.56		1140000	Cristina Lopes
NE Pacific	Y6711-5	42.40	-124.90		17500000	Cristina Lopes
NE Pacific	Y6706-7	42.50	-124.70		1420000	Cristina Lopes
NE Pacific	Y6708-38	42.59	-124.84		18700000	Cristina Lopes
NE Pacific	W7905A-167G arch	42.66	-124.93		11800000	Cristina Lopes
NE Pacific	Y6708-42	42.70	-124.62		549000	Cristina Lopes
NE Pacific	Y6706-8	42.82	-124.81		1770000	Cristina Lopes
NE Pacific	W8508-9GC	43.00	-126.60	3092	8740000	Cristina Lopes
NE Pacific	W7905-160G	43.20	-125.10	1476	5860000	Cristina Lopes

Location	Station	Latitude (S -; N +)	Longitude (W -; E +)	Depth (m)	SDA (#valves/g)	Author / Counting Method
NE Pacific	W7905-163G	43.20	-124.80	308	2290000	Cristina Lopes
NE Pacific	7407Y-1 REF	43.60	-127.10	2918	14300000	Cristina Lopes
NE Pacific	W9205-1GC	44.10	-125.40	3020	6770000	Cristina Lopes
NE Pacific	W7610B1-7MGREF	44.20	-126.20	2893	675000	Cristina Lopes
NE Pacific	W7905A-106 GC	44.23	-124.66	522	273000	Cristina Lopes
NE Pacific	W8909ABC	44.70	-125.30		8480000	Cristina Lopes
NE Pacific	W8306-A1-RKC*	44.90	-125.40	2511	28100000	Cristina Lopes
NE Pacific	AT9009-2 GC	45.14	-125.44	2650	2550000	Cristina Lopes
NE Pacific	Y7409-15 24GC	46.10	-124.10	200	5160000	Cristina Lopes
NE Pacific	W7905-109G	46.30	-125.10	1670	591000	Cristina Lopes
NE Pacific	TT68-PC 27 REF	46.40	-126.10	2050	10000000	Cristina Lopes
NE Pacific	TT29-18 PC	46.43	-128.38	2742	189000	Cristina Lopes
NE Pacific	TT063-12	46.70	-125.00		1360000	Cristina Lopes
NE Pacific	TT39-5AC REF	46.70	-127.50	2665	11600000	Cristina Lopes
NE Pacific	Y6908-5A	46.70	-129.10	2600	4260000	Cristina Lopes
NE Pacific	TT31-011 GC REF	47.00	-131.20	3056	3400000	Cristina Lopes
NE Pacific	TT29-22 AC REF	47.10	-127.90	2555	7220000	Cristina Lopes
NE Pacific	AT8408-17	47.20	-126.10	2390	7520000	Cristina Lopes
NE Pacific	TT68-18 AC	47.40	-124.90	1240	3040000	Cristina Lopes
NE Pacific	TT39-22 PC	47.59	-129.51	2566	1140000	Cristina Lopes
NE Pacific	TT39-23 PC	47.63	-128.67	2625	560000	Cristina Lopes
NE Pacific	TT39-21 AC	48.06	-128.06	2575	1640000	Cristina Lopes
NE Pacific	TT90-33 GC	48.10	-126.02	1474	973000	Cristina Lopes
NE Pacific	TT39-17 PC	48.23	-130.03	2793	631000	Cristina Lopes
NE Pacific	TT39-19 REF	48.40	-127.20	2555	1710000	Cristina Lopes
NE Pacific	TT39-18 AC REF	48.40	-129.90	2765	12800000	Cristina Lopes
NE Pacific	TT39-11 AC REF	49.00	-127.80	2480	13500000	Cristina Lopes
NE Pacific	TT39-15 REF	49.20	-129.20	2396	9440000	Cristina Lopes
NE Pacific	TT39-AC12REF	49.40	-128.10	2341	16000000	Cristina Lopes

SI Table 2

Values estimated using the Log curve fit to the data

	All Areas	Nhemisphere	NH no Indian	SHemisphere	Atlantic	Pacific	Indian
DiatMAX	4.10E+08	4.78E+06	7.52E+06	3.00E+07	1.66E+06	2.81E+08	2.21E+08
SisurfMAX	6.978	12.028	12.05	6.978	6.695	6.978	9.486
DiatS	1.61E+05	6.67E+04	1.61E+05	1.66E+05	3.98E+05	5.49E+05	1.64E+06
SisurfS	1.845	1.533	0.657	2.393	0.657	2.2912	3.65
$V = V_{\max} [S] / (K_s + [S])$							
Increase by μM Sisurf	3.E+08	4.E+06	7.E+06	2.E+07	2.E+06	2.E+08	2.E+08

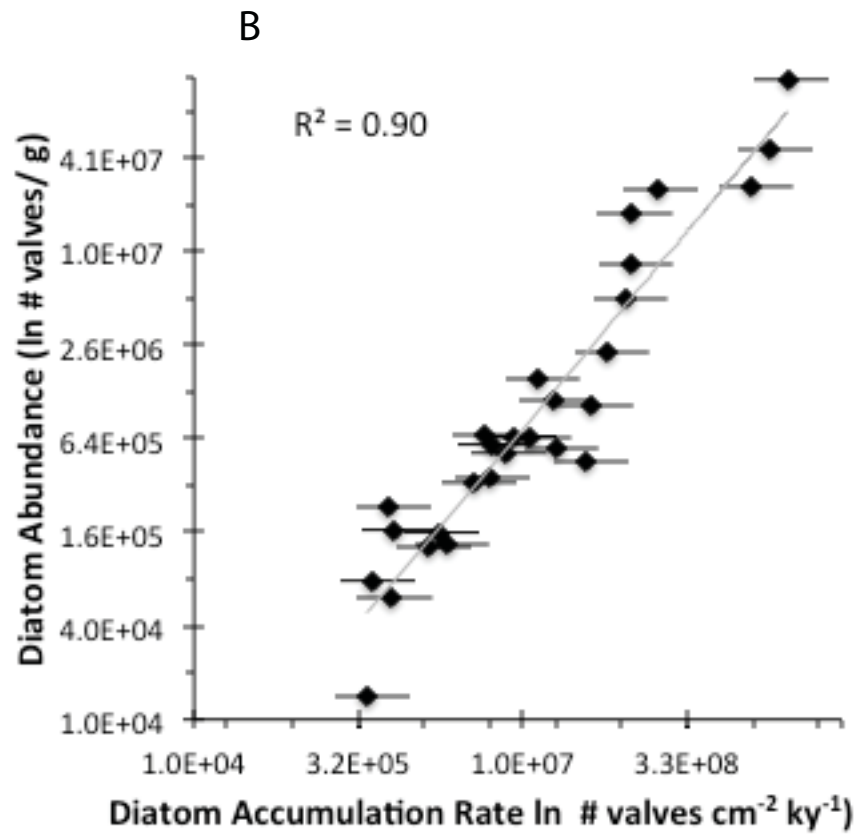
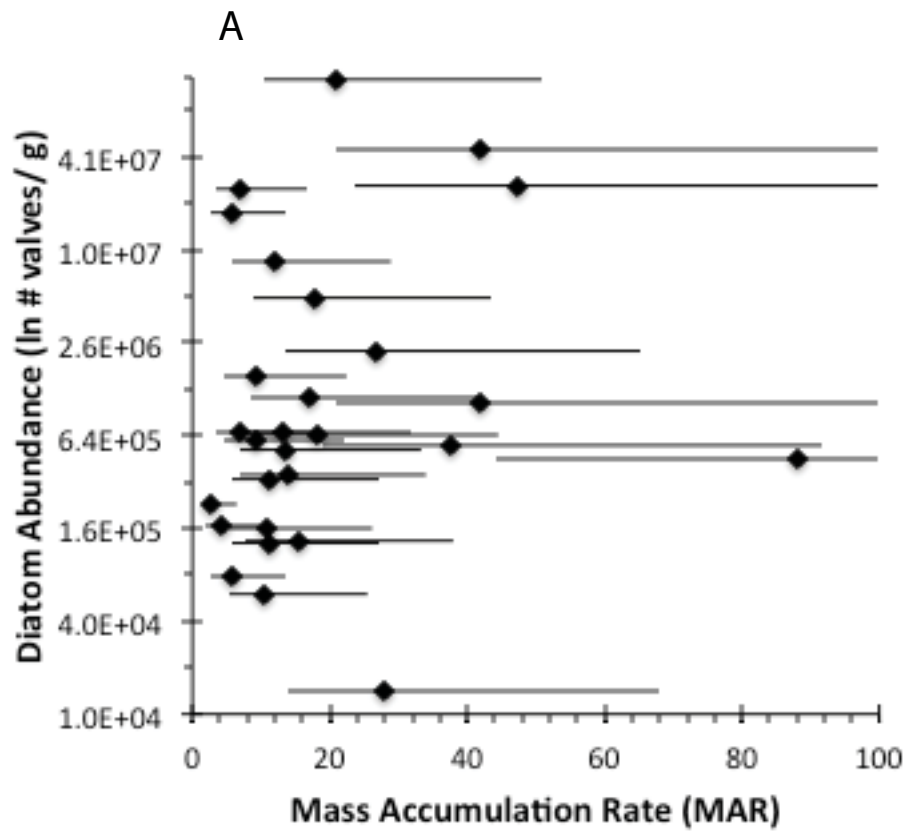
SI Table 3

ID	Latitude	Longitude	Depth (m)	SR (cm/ky)	Reference
Galiza					
11002-1	42.17	-8.99	111	63.0	(1)
11039-1	41.55	-9.08	99	27.0	(1)
PM					
2979 - PO8-2	37.64	-9.93	2200	19.2	(2)
3010 - PO28-1	41.49	-9.72	2160	7.5	(2)
3082 - MD95-2042	37.8	-10.17	3146	20.0	(3)
3104- MD95-2040	40.58	-9.86	2465	11.2	(4)
NW Africa					
M4216-1	30.63	-12.4	2324	5.0	(5)
M4223-1	29.02	-12.47	777	9.8	(5)
M4228-1	29.47	-12.99	1633	4.0	(5)
GeoB7926-1	20.21	-18.45	2500	12.2	(6)
GeoB7920-3	20.75	-18.58	2278	11.5	(7)
SW Africa					
GeoB1704-1	-19.41	11.62	399	8.0	(8)
GeoB1705-2	-19.50	11.38	647	13.1	(8)
GeoB1707-2	-19.70	10.66	1234	9.4	(9)
GeoB1711-4	-23.32	12.37	1975	10.0	(10)
GeoB1712-1	-23.25	12.81	1004	8.0	(11)
GeoB1718-1	-28.71	15.21	167	7.7	(12)
GeoB1719-4	-28.93	14.17	1023	6.5	(9)
GeoB1720-4	-29.00	13.84	2004	4.0	(13)
GeoB1721-4	-29.18	13.09	3079	2.9	(14)
GeoB1722-3	-29.45	11.75	3074	1.9	(14)
GeoB3606-1	-25.47	13.08	1793	30.0	(9)
SE Pacific					
RR9702A-74	-16.24	-76.24	3 476	4.9	(15)
ME005A-21	0.02	-86.46	2 942	12.8	(15)
NE Pacific					
W8709A13PC	42.10	-125.80		30.0	(16)
Oman					
NIOP 905	10.81	52.13	3540	33.9	(17)
RC 2714	18.25	57.66	4040	15.0	(18)
RC 2761	16.66	59.86	455	8.5	(19)

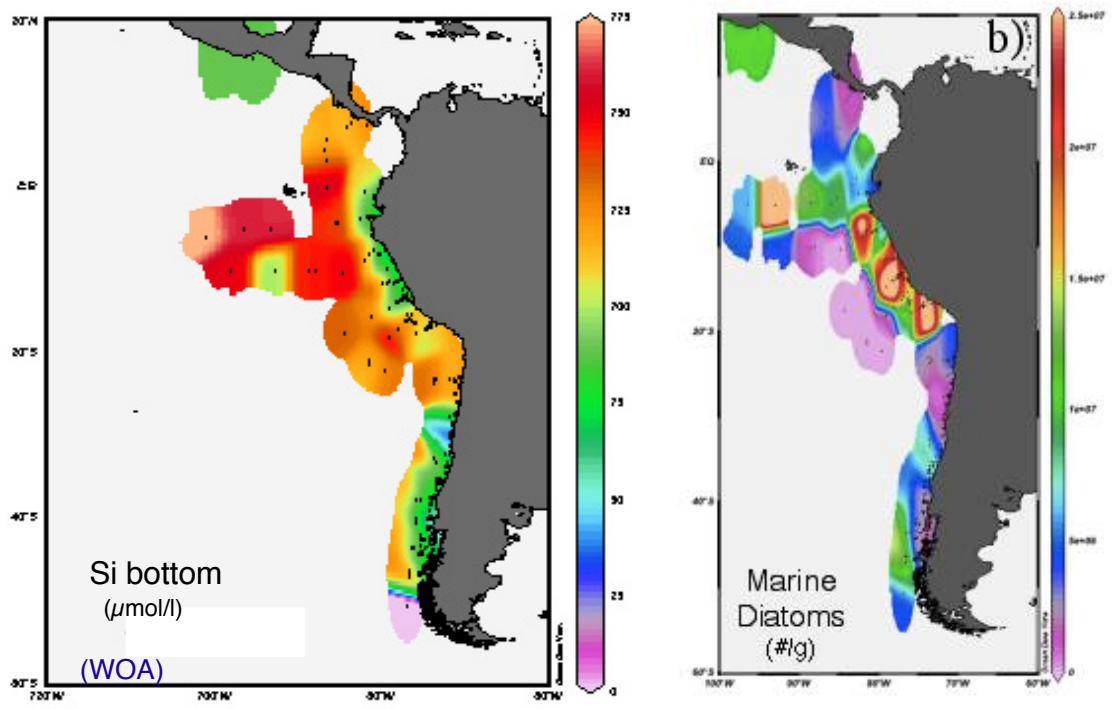
REFERENCES

1. Lantzsch H, Hanebuth T, & Bender V (2009) Holocene evolution of mud depocentres on a high-energy, low-accumulation shelf (NW Iberia). *Quaternary Research* 72:325-336.
2. Abrantes F, *et al.* (1998) Hydrographic changes along the European Margin between 20 and 8 kyrs: Sediment Fluxes. *Marine Geology* 152(1-3):7-24.
3. Shackleton N (2000) The 100,000-Year Ice-Age Cycle Identified and Found to Lag Temperature, carbon Dioxide, and Orbital Eccentricity. *Science* 286:1897-1902.
4. Abreu Ld, Shackleton NJ, Schonfeld J, Hall M, & Chapman M (2003) Millennial-scale oceanic climate variability off the Western Iberian margin during the last two glacial periods. *Marine Geology* 196:1-20.
5. Henderiks J, *et al.* (this volume) Glacial-interglacial variability of particle accumulation in the Canary Basin: A time-slice approach. *Deep-Sea Research*.
6. McKay C, Filipsson H, Romero O, Stuut J-B, & Donner B (2014) Pelagicebenthic coupling within an upwelling system of the subtropical northeast Atlantic over the last 35 ka BP. *Quaternary Science Reviews* 106(106):299-315.

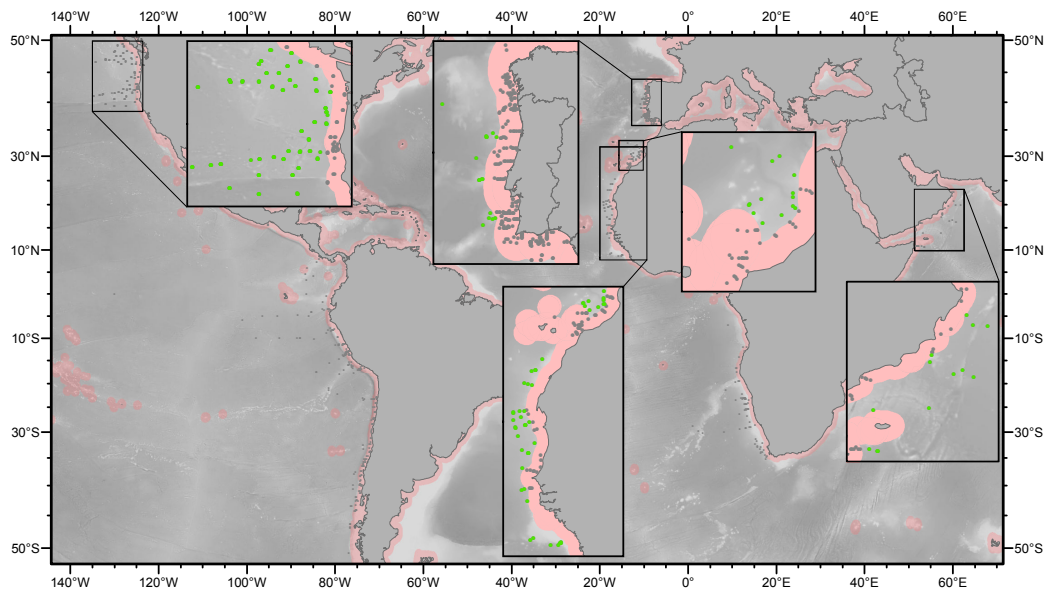
7. Tjallingii R, *et al.* (2008) Coherent high- and low-latitude control of the northwest African hydrological balance. *Nature Geosci* 1:670-675.
8. Mollenhauer G, *et al.* (2007) Aging of marine organic matter during cross-shelf lateral transport in the Benguela upwelling system revealed by compound-specific radiocarbon dating. *Geochem. Geophys. Geosyst.* 8(Q09004).
9. Mollenhauer G, Schneider, R. , Müller, P. , Spieß, V. and Wefer, G. (2002) Glacial/interglacial variability in the Benguela upwelling system: Spatial distribution and budgets of organic carbon accumulation *Global Biogeochem. Cycles* 8(Q09004).
10. Kirst G, Schneider R, Muller P, von Storch I, & Wefer G (1999) Late Quaternary temperature variability in the Benguela Current system derived from alkenones. *Quaternary Research* 52(1):92-103.
11. Kim J-H & et a (2002) Interhemispheric comparison of deglacial sea-surface temperature patterns in Atlantic eastern boundary currents. *Earth and Planetary Science Letters* 194:383-393.
12. Mollenhauer G, Eglinton TI, Hopmans EC, & Sinninghe Damsté JS (2008) A radiocarbon-based assessment of the preservation characteristics of crenarchaeol and alkenones from continental margin sediments *Organic Geochemistry* 39(8):1039-1045.
13. MOLLENHAUER G, *et al.* (2003) Asynchronous alkenone and foraminifera records from the Benguela Upwelling System. *Geochimica et Cosmochimica Acta* 67(12):2157-2171.
14. Mollenhauer G, Schneider R, Jennerjahn T, Müller P, & Wefer G (2004) Organic carbon accumulation in the South Atlantic Ocean: Its modern, mid-Holocene and Last Glacial distribution *Global and Planetary Change* 40:249-266.
15. Reimers C & Suess E (1983) Late Quaternary fluctuations in the cycling of organic matter off central Peru: A proto-kerogen record. *Coastal Upwelling Its Sediment Record*, ed Suess JTaE (Plenum-Press).
16. Lopes C & Mix A (2009) Pleistocene megafloods in the northeast Pacific. *Geology* 37:79-82.
17. Jung S, Kroon D, Ganssen G, Peeters F, & Ganeshram R (2009) Enhanced Arabian Sea intermediate water flow during glacial North Atlantic cold phases. *Earth and Planetary Science Letters* 280:220-228.
18. Altabet M, Higginson M, & Murray DW (2002) The effect of millennial-scale changes in Arabian Sea denitrification on atmospheric CO₂. *Nature* 415:159-162.
19. Clemens SC & Prell WL (1991) Late Quaternary Forcing of Indian Ocean Summer-Monsoon Winds : A Comparison of Fourier Model and General Circulation Model Results. (Am.Geophysical Union), pp 22,683-622,700.



SI Figure 1

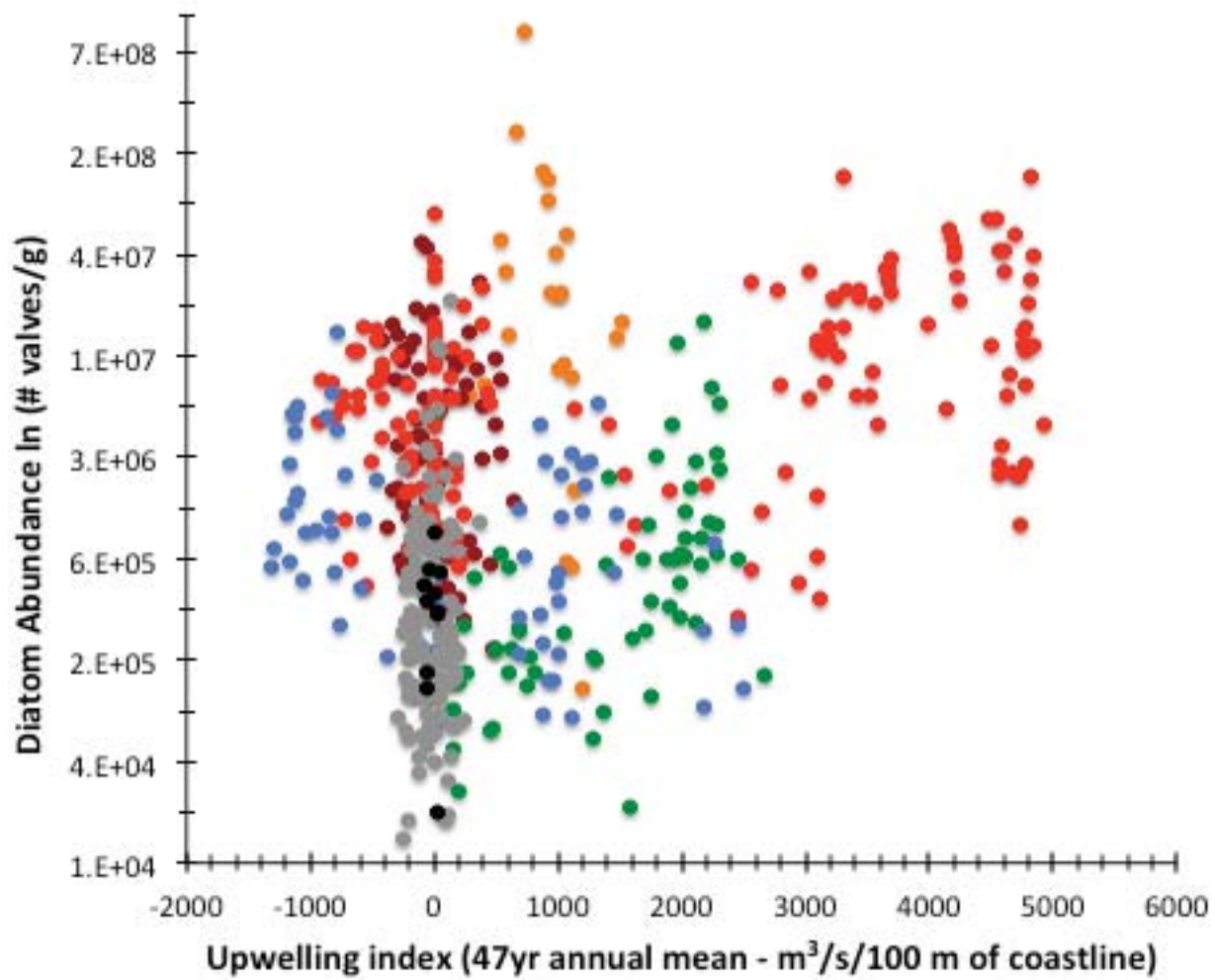


SI Figure 2

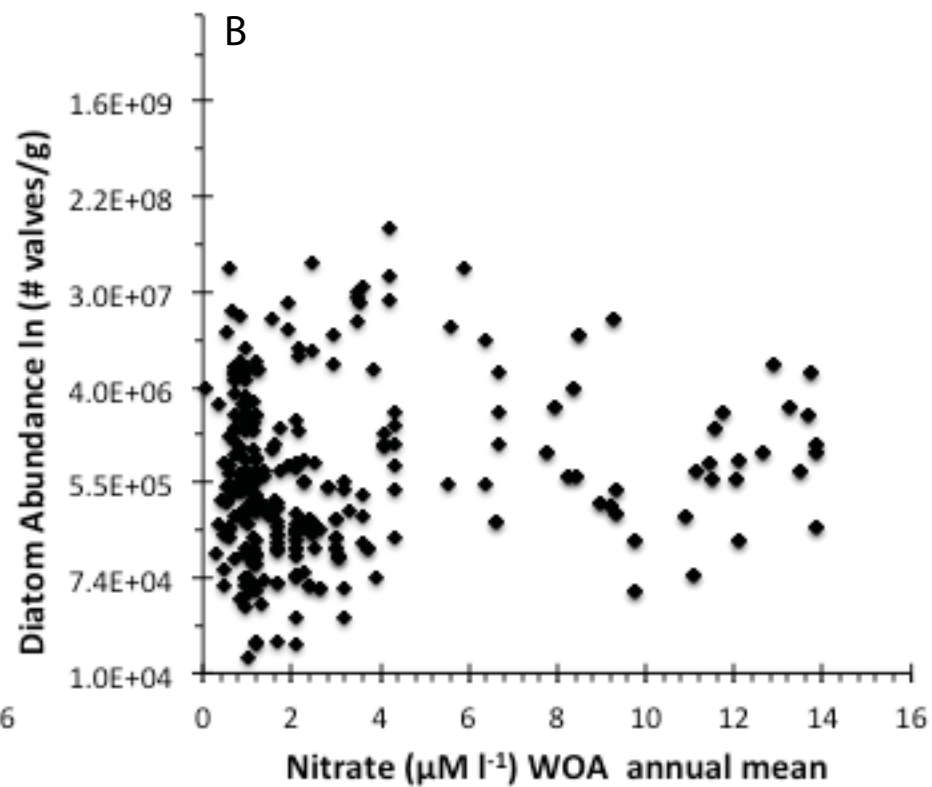
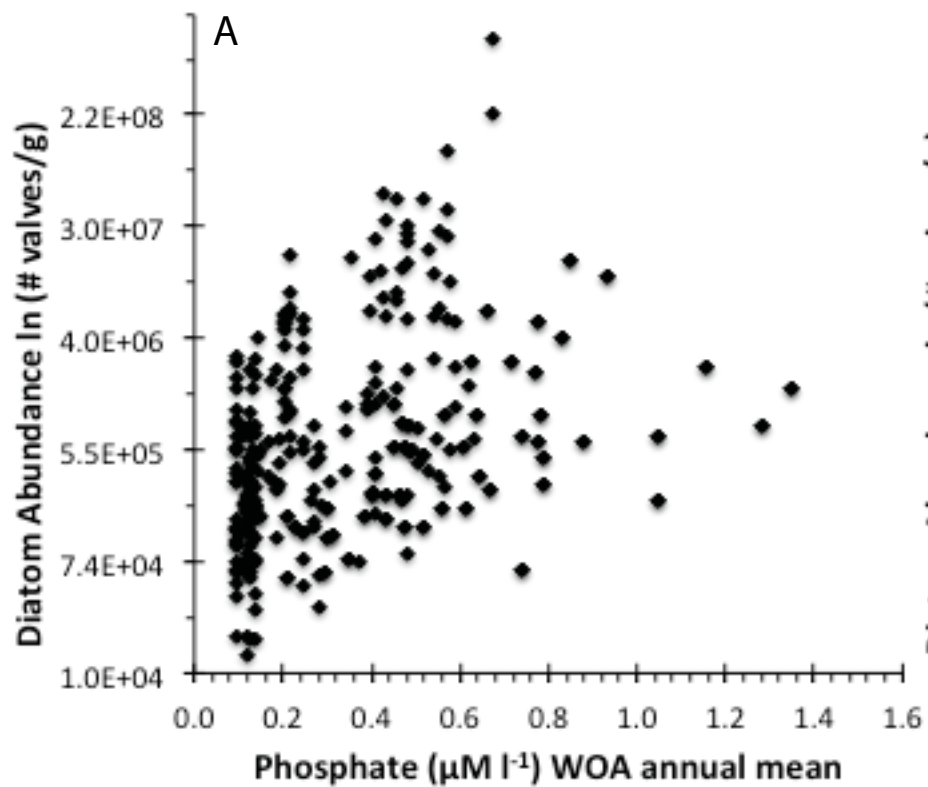


Document Name: NOAA satellite data retrieval for Dra Fatima_with Insets_and 1DD buffer analysis
Document Path: D:\DATA\GIS\Maps\Other Projects\13 - Dra Fatima NOAA WOA\NOAA satellite data retrieval for Dra Fatima_with Insets_and 1DD buffer analysis.mxd

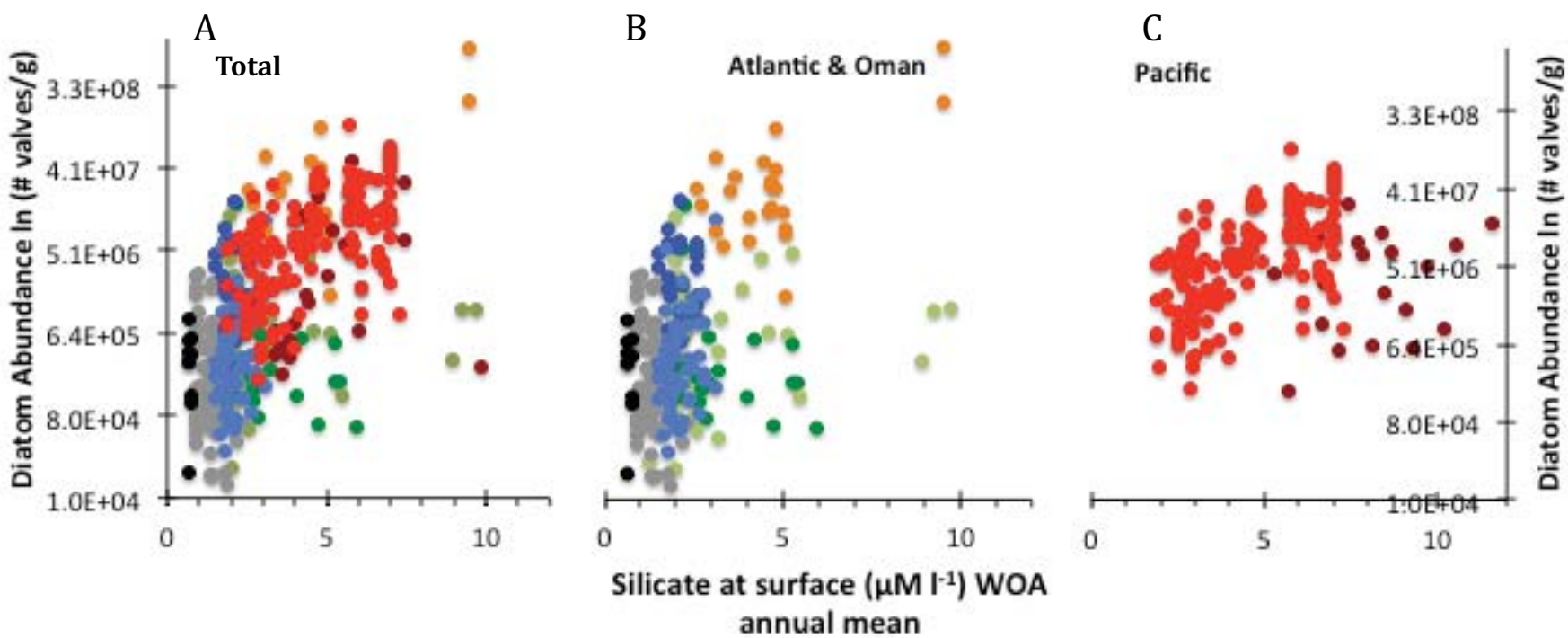
SI Figure 3



SI Figure 4



SI Figure 5



SI Figure 6